UC Berkeley
UC Berkeley Previously Published Works

Title

The Technical and Energetic Challenges of Separating (Photo)Electrochemical Carbon Dioxide Reduction Products

Permalink

Journal

ISSN

Authors

Greenblatt, Jeffery B
Miller, Daniel J
Ager, Joel W
et al.

Publication Date

DOI

The technical and energetic challenges of separating (photo)electrochemical carbon dioxide reduction products

Jeffery B. Greenblatt,[1,*] Daniel J. Miller,[1] Joel W. Ager,[1] Frances A. Houle,[1] Ian D. Sharp[2]

[1] Joint Center for Artificial Photosynthesis, Lawrence Berkeley National Laboratory, Berkeley, CA 94720, USA

[2] Walter Schottky Institut and Physik Department, Technische Universität München, Garching, Germany

* To whom correspondence should be addressed: jbgreenblatt@lbl.gov, +1 (415) 814-9088

Draft date: December 21, 2017

Table of Contents

Abstract

Known catalysts for (photo)electrochemical carbon dioxide (CO_2) reduction typically generate multiple products, including hydrogen, carbon monoxide, hydrocarbons and oxygenates, making product separation a ubiquitous, yet often overlooked, challenge. Here we review observed and expected CO_2 reduction products using available catalysts, and discuss the range of possible approaches for product separation, including distillation, solvent extraction, membranes and other techniques, along with estimates of separation energy requirements. We illustrate potential complexities in a multi-step separation process for products of CO_2 reduction on copper, and discuss opportunities to minimize separations by utilizing product mixtures. To consider the full system energy balance, we also examine potential CO_2 sources, their energy requirements and net CO_2 emissions. Finally, we discuss driving separations using energy available from waste sources, and integrate this information into an overall energy balance assessment. Using a common renewable energy sustainability metric, energy return on energy investment (EROEI), we find that an EROEI of ~2.0 may be possible, before including separation and CO_2 production energy inputs. Therefore, for net energy to remain above the break-even point (e.g., EROEI > 1), these additional energy requirements, including the embodied energy of equipment, must be no greater than approximately half of the product energy output, though the use of waste energy to drive separations could relax this limitation.

Keywords

carbon dioxide reduction; solar fuels; low-carbon fuels; green fuels; solar energy; artificial photosynthesis; climate change; greenhouse gas; electrochemistry; photoelectrochemistry; catalysis; photocatalysis; product separation; energy return on energy investment; sustainability; net energy balance

1   Introduction

1.1   The fuels challenge

With adoption of the Paris Agreement (UNFCCC, 2015), many nations are committed to dramatic reductions in greenhouse gas (GHG) emissions across economic sectors over the next several decades. As ~80% of total radiative forcing arises from anthropogenic atmospheric carbon dioxide (CO_2) (Myhre et al., 2013) that largely results from fossil fuel combustion, it is essential to either greatly reduce the use of fossil fuels, lower their net GHG emissions, or both. More efficient energy use is the cornerstone of almost all climate policy (IEA, 2015). While many low-GHG energy alternatives exist for electricity generation, including several types of renewable technologies as well as nuclear power and fossil fuel combustion with CO_2 capture and sequestration (CCS) (Greenblatt et al., 2017), there are fewer options available for fuels used directly (e.g., in transportation, buildings or industrial processes). Electrification of these end

uses is underway, most prominently in personal vehicles where plug-in hybrid gasoline-electric, diesel-electric and all-electric technologies are rapidly becoming cost-effective. Several regions, including California (Multi-State ZEV Task Force, 2014; CARB, 2017), France (Ewing, 2017a), the United Kingdom (New York Times, 2017), China (Liptak, 2017; Zhang, 2017) and at least one conventional automobile manufacturer (Ewing, 2017b), have committed to a great expansion in their use, with more than two million such vehicles already in existence globally (CARB, 2017). Building and industrial electrification are also receiving increased attention (E3, 2015).

Despite encouraging progress towards alternatives, the need for energy-dense fuels will remain strong for many decades and perhaps indefinitely. Global energy demand is forecast to increase 32% by 2040 even under the pressure of the Paris Agreement (IEA, 2015), though demand shifts away from the U.S. and other developed countries and toward China, India, southeast Asia, and parts of Africa, Latin America and the Middle East. Despite efforts to reduce GHG emissions, demand for natural gas is expected to grow by 46% to 178 exajoules (EJ) globally in 2040, with major uses in power generation (40%), industry (22%) and buildings (18%). Even in the International Energy Agency (IEA)'s aggressive 450 Scenario, which reflects climate policy needs under the Paris Agreement, natural gas demand in 2040 would be 140 EJ (IEA, 2015). Oil is projected to grow by 12%, reaching 198 EJ by 2040 under the IEA's reference scenario, whereas in the 450 Scenario, oil demand would fall to 140 EJ in 2040, with demand concentrating in freight, aviation and petrochemical uses. However, gasoline demand remains important: electric vehicles, despite tremendous forecast growth to 715 million in 2040 in the 450 Scenario, only reduces oil demand by 13 EJ, or <10% (IEA, 2016), and biofuels are projected to contribute 19 EJ in 2040, with hydrogen (H_2) playing an insignificant role. Thus, despite the rapid projected growth of alternatives, there will remain a huge need for fossil fuel substitutes.

1.2   Challenges and opportunities for (photo)electrochemical products

While several methods exist for producing H_2, carbon monoxide, hydrocarbons and/or oxygenates (hereafter "fuels") without using fossil feedstocks, including biological (e.g., Bensmann et al., 2014) and thermochemical (e.g., Tou et al., 2017) methods, electrochemical (EC) and photoelectrochemical (PEC) routes offer potentially transformative technologies that could scale globally, with fewer inefficiencies and less land competition than are associated with biomass-based products. A number of reviews have highlighted the importance of these technologies (e.g., Graves et al. 2011; Newman et al., 2012; van der Giesen et al., 2014; Herron et al., 2015; Kumar et al., 2016). Promising progress has been demonstrated for solar H_2 from water splitting (Rongé et al., 2014; Ager et al., 2015; Bonke et al., 2015; Jia et al., 2016; Shi et al., 2016), though many challenges remain. However, carbon-based fuel production requires both the reduction of CO_2 and the oxidation of water, and is a far more challenging undertaking than the H_2 production alone. A conceptual schematic of a PEC or EC (hereafter P/EC) CO_2 reduction system is shown in Figure 1, and several characteristics are described in this section.
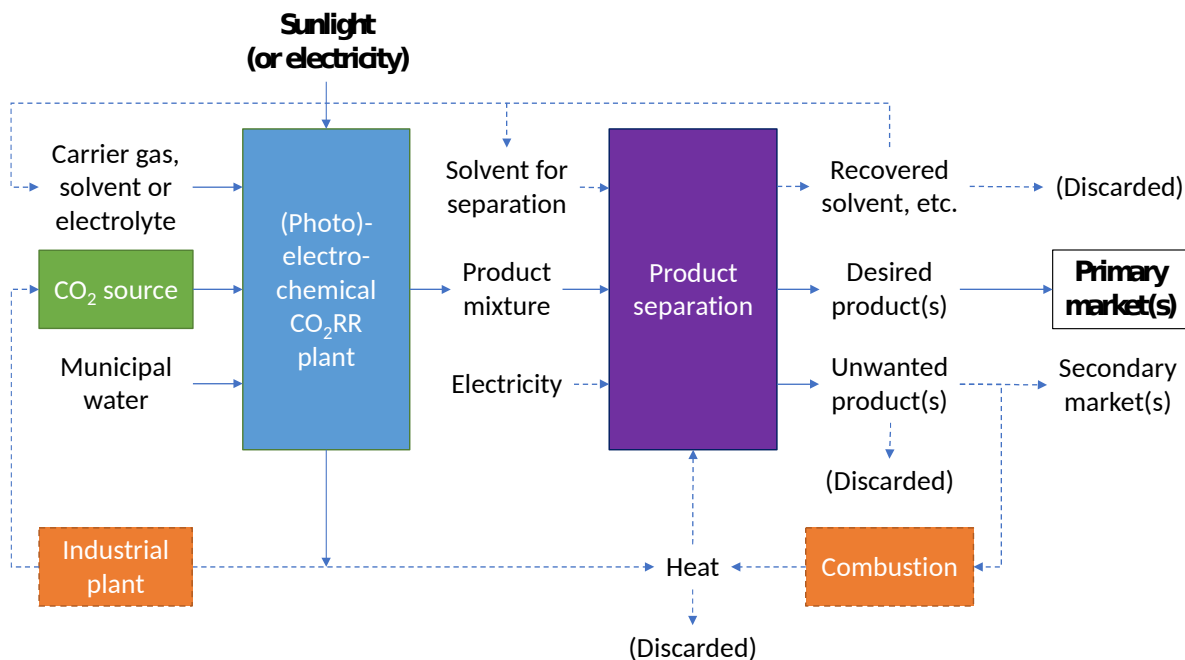
Figure 1. Conceptual diagram of P/EC CO₂RR system including CO₂ source, CO₂RR plant, product separation, waste heat utilization, and recovery of carrier gas, solvent or electrolyte. Solid and dashed lines indicate definite and possible pathways, respectively.

Most desirable CO_2 reduction reaction (CO_2RR) fuel products are the result of greater than two-electron reduction processes, which tend have relatively low overall efficiencies. Few CO_2RR catalysts capable of four or more electron reduction reactions currently exist, so the range of products available in appreciable yields is quite limited. While electrochemical potentials of most CO_2RR (–1.06 to –1.40 V vs. standard H_2 electrode) are similar to water splitting (–1.23 V), with the exception of CO and formate most require significant (~1.0 V) kinetic overpotentials to drive product formation. Large photovoltages are required to generate such products in integrated photoelectrochemical reactors. For single absorber configurations, large photovoltages necessitate large bandgap semiconductors that can only absorb the short wavelength portion of the solar spectrum, resulting in very low solar-to-fuel efficiencies. Thus, in most cases, multiple photoabsorber configurations, such as tandem photovoltaics coupled to appropriate catalysts, are used to provide the requisite voltage to PEC systems (Rongé et al., 2014). For EC cells, a series-connected photovoltaic array could be used to provide the requisite voltage at high efficiency (Jia et al., 2016; Schüttauf et al., 2016).

CO_2RR catalysts typically yield a mixture of products, making product separation a ubiquitous, yet often overlooked, challenge. In addition, product distributions can vary with light intensity (Zhou et al., 2016), and designing a system with stable product output is an additional challenge (Gurudayal et al., 2017). CO_2 solubility in water is low, so alternative approaches such as non-aqueous solvents, elevated pressures, gas phase reactions and even decoupling of light capture and catalysis are important to explore. Moreover, unlike water, which is widely available in relatively pure form, obtaining a reasonably pure source of CO_2 is much more challenging. While it is present in the atmosphere at ~400 ppm, this source is very dilute and hence energy-intensive to concentrate. While CO_2 can be captured from more concentrated sources (e.g., industrial flue

gases), these sources are associated with appreciable GHG emissions, which diminish their value in mitigating climate change. These and other CO_2 sources, including several with very low net GHG emissions, are discussed in Section .

Despite these challenges, CO_2RR also provides several opportunities not available from water splitting. Most carbon-containing fuels are easier to store than H_2, which requires energy to pressurize (including to a liquefied gas), and special materials for storage and transport that are impervious to H_2 permeation and do not embrittle. Liquid carbon-containing fuels are also much more energy dense than even liquid H_2 on a volume basis, and are therefore convenient for transportation and other space-constrained applications. Many P/EC CO_2RR products (CH_4, C_2-C_4 gases,[×] ethanol/gasoline mixtures, and gasoline from methanol; these are discussed in detail in Section 2) as well as small amounts of H_2 are compatible with existing infrastructure. Other fuels might require only small changes in existing infrastructure (e.g., dimethyl ether substitute for diesel, which requires either cooling to –24 °C or pressurization to ~5 bar to liquefy) (Wei et al., 2014).

CO_2 reduction could, in principle, provide unlimited quantities of near-net zero GHG emissions fuels without requiring biomass. As such, it would not be limited by suitable agricultural land, transport of diffuse feedstocks, conversion of biomass feedstocks to finished products, or low overall solar-to-product efficiency. EC CO_2 reduction could also provide an important enabling technology for future electricity systems with low GHG emissions through the conversion of inexpensive electricity, typically when net supply from intermittent renewable generation exceeds demand, into storable products ("power-to-gas"). These systems are currently being envisioned as EC water-splitting devices with subsequent conversion to CH_4 via the Sabatier reaction or biological routes. Such systems have been demonstrated on scales up to 6 MW (Benjaminsson et al., 2013).

The energy return on energy investment (EROEI) ratio is a key sustainability metric for renewable energy technologies (Pimentel, 2003; de Oliveira et al., 2005; Gupta and Hall, 2011; Sathre et al, 2014, 2016; Armaroli and Balzani, 2016; Shaner et al., 2016). As shown in Figure 1, two types of processes have to be considered for EROEI analyses of CO_2 reduction systems: CO_2 reduction reaction and product separation. Rather than address, as others have, the P/EC CO_2RR itself, we will focus in this paper on EROEI of product separation technologies including their required energy inputs and the embodied energy of equipment, solvents and other materials necessary for plant operation. Separations, which are usually overlooked, represent one of the most significant challenges for such a system, because unlike water reduction, which produces only H_2 and oxygen (O_2) gases that are relatively easily separated from aqueous solution and from each other, P/EC CO_2RR typically produces a range of gaseous and liquid products. These separations require energy, potentially negating the energy benefits of using sunlight or renewable electricity to reduce CO_2 to high energy density products. Importantly, current separations technologies define the availability of useful products, and the prospects for improved separations define possible useful products in the future. Likewise, the availability of selective catalysts for specific products (or classes of products) that are readily separated can guide future basic research in materials and systems for separations. In this way, analyses such as

---

Here we adopt the notation C_n to indicate molecules with n carbon atoms.

those presented here can facilitate an interaction between catalysis and separations researchers in order to progress toward science solutions for the challenges solar fuels production.

1.3 Target products from CO_2 reduction

Global consumption of fuels is dominated by transportation and heating uses (Figure 2). While natural gas is the largest single demand category, the demand (as measured by energy content) for all petroleum products combined exceeds that of natural gas by a considerable margin. The top six commodity chemicals are shown on the bottom portion of Figure 2, and are consumed in far smaller quantities than transportation fuels. Ethanol and biodiesel, the primary two biofuels, together contribute less than 2 EJ to the nearly 300 EJ consumed annually.
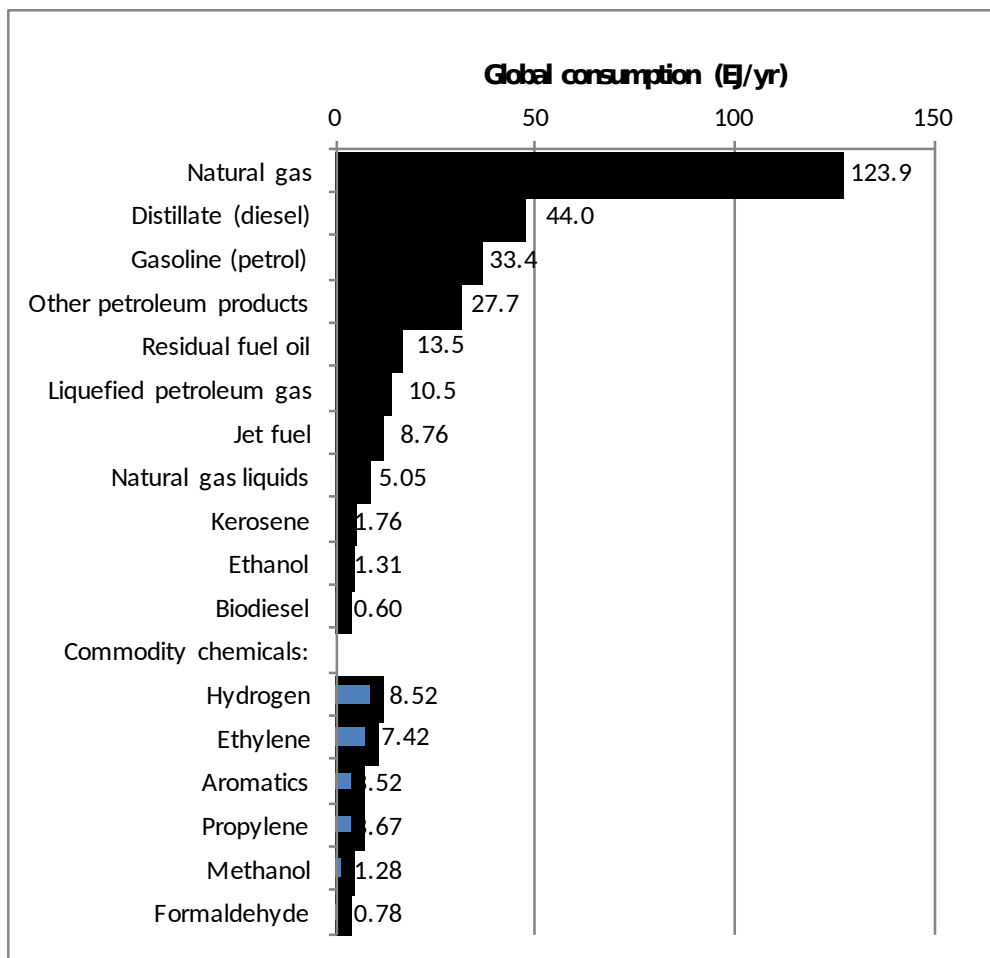
Figure 2. Global fuel and commodity chemical consumption in 2012. Sources: Badwal (2013), Bender (2013), Goeppert et al. (2014), Indexmundi (2017), MRC (2014), Research and Markets (2016)

While the production of each additional EJ of low-GHG fuels from CO_2 would be a significant contribution, a 10% reduction in global (fossil) fuel demand would require ~30 EJ annually. Therefore, the substitution of a CO_2RR product for a fossil-generated product with a small global demand does not constitute a globally-scalable GHG reduction solution. Fuel substitutes would be most impactful in the following categories:

- Natural gas (primarily methane, CH_4): 124 EJ/yr
- Diesel (C_{10}-C_{15} saturated hydrocarbons; approximately dodecane); jet fuel and kerosene have similar structures, but with slightly longer chain lengths: 55 EJ/yr combined.
- Gasoline (C_4-C_{12} saturated hydrocarbons; approximately octane) and aromatics (benzene, toluene and xylenes, C_6-C_8): 37 EJ/yr combined.
- Short-chain (C_2-C_3) hydrocarbons, consisting of ethane (C_2H_6), ethylene (C_2H_4), propane (C_3H_8), and propylene (C_3H_6). Both liquefied petroleum gases (LPG) and natural gas liquids consist primarily of these chain lengths, but also contain some longer chain molecules (C_4-C_5 and sometimes higher). Natural gas liquids mixtures tend to contain longer-chain hydrocarbons than LPG, and do not include unsaturated molecules (e.g., C_2H_4 and C_3H_6): 35 EJ/yr combined.

Information about commodity costs of fuels can be found in Section 1 of the Supplemental Information.

2 CO_2RR products

There is a significant gap between products for which there is high demand, and what is currently known to be possible using available catalysts. In this section, we consider only products that have been reported to have been formed by EC reduction of CO_2 in aqueous solution or in a gas diffusion electrode (GDE) cell, and describe their uses and physical characteristics. It should be mentioned that there are other pathways for forming carbon-containing fuel products from CO_2 including those that use renewable H_2 and Fischer-Tropsch synthesis (Centi and Perathoner, 2014), but these are beyond the scope of the present study.[×] The main advantage of a GDE reactor over an aqueous reactor is that CO_2 generally exists at higher concentration in the vapor phase than when dissolved in water, but in both types of reactors, reduction products are generated in a flowing aqueous electrolyte stream saturated with CO_2, and thus are likely to be present at low concentrations if the flow rate is high relative to the production rate. At high product concentrations, the product will separate from the aqueous electrolyte according to its solubility in the electrolyte. If the product solubility in the aqueous electrolyte is high, additional separation processes are required to remove dissolved CO_2 and organic products from the electrolyte, and to separate organic mixtures into components.

Surveying the current state-of-the-art in CO_2RR electrocatalysis (Centi and Perathoner, 2010; Li, 2010; Kuhl et al., 2012; Costentin et al., 2013; Jhong et al., 2013; Qiao et al., 2014; Goeppert et

---

[×] Fischer-Tropsch synthesis can be used to effectively convert easy-to-produce reagents (H_2 and CO) into long-chain hydrocarbons including those directly compatible with gasoline-, diesel- or jet fuel-burning engines. Another advantage of the approach is that it is exothermic, requiring in principle no additional energy inputs. However, the Fischer-Tropsch approach must be carried out at temperatures of 150-350 °C and typically elevated pressures (up to 30 atm), requires additional catalysts and large amounts of physical hardware, and often relies on significant downstream processing (Schulz, 1999; https://www.netl.doe.gov/research/coal/energy-systems/gasification/gasifipedia/ftsynthesis).

al., 2014; Ganesh, 2014; Lim et al., 2014; Jones et al., 2014; Kumar et al., 2016; Zhou et al., 2016), the following general observations can be made:

- EC CO_2RR can only make C_1-C_3 products with appreciable Faradaic efficiency (Section 2 of the Supplementary Information contains a list of all possible products), although a few studies have indicated the possible production of products with four or more carbon atoms (e.g., Centi et al., 2007; Shibata et al., 2008).
- Certain C_1 products, such as CO and formate, can be made with high selectivity, but selectivity to C_2 products such as C_2H_4 and/or ethanol remains poor.
- For some catalysts that produce C_{2+} products, the product distribution depends sensitively on current density (and hence light intensity in a directly solar-coupled system).

2.1 Carbon monoxide

It has been well demonstrated since the 1980s that metal electrodes such as gold and silver are able to reduce CO_2 to CO with high Faradaic efficiency (Hori, 2008). Recently, nanostructured versions of these metals have been shown to produce CO at low overpotential (<200 mV) (Chen et al., 2012; Tornow et al., 2012). A number of studies have utilized these types of catalysts in a GDE geometry at current densities exceeding 100 mA/cm^2 (Delacourt and Newman, 2010; Delacourt et al., 2010; Kim et al., 2015). Moreover, a techno-economic case has been made for using this process as the first step to renewable fuel production, with the subsequent steps performed with the Fischer-Tropsch process (Newman et al., 2012).

While CO may be useful, it is also a toxic gas with low energy density relative to other gaseous products (e.g., CH_4). CO could be an important component of syngas (along with H_2) as an intermediate step to making long-chain hydrocarbons, such as gasoline or diesel, via Fischer-Tropsch.

2.2 Formate/formic acid

Tin and indium can produce formate[×] with high Faradaic efficiency (Hori, 2008; Bumroongsakulsawat and Kelsall, 2014), and nanostructuring has been shown to be effective in reducing overpotentials (Zhang et al., 2014). CO_2 reduction to formate has been demonstrated in a number of GDE cells (Wang et al., 2015; Del Castillo et al., 2014; Kopljar et al., 2014; Irtem et al., 2016; Machunda et al., 2011; Li and Oloman, 2005; Prakash et al., 2013). Recently, Zhou et al. (2016) demonstrated a coupled PEC water oxidation and CO_2RR that produces formate at 10% solar-to-fuel efficiency.[×]

All known catalysts operate efficiently only under basic conditions, where they produce formate rather than formic acid, but the hydrocarbon portion of the two compounds are identical.

This metric is defined as the chemical energy (absolute enthalpy of combustion as measured on a higher heating value basis) of the produced fuel divided by the energy of the standard solar spectrum (defined as AM1.5G; NREL, no date) striking the photoabsorber surface.

While this work is promising from an energy conversion point of view, formate has limitations as a fuel product. Formic acid has the lowest energy density per mole or kg of any fuel, lower even than CO. It could potentially be used in a fuel cell or as an efficient H_2 carrier (Pérez-Fortes and Tzimas, 2016). Indeed, pure formic acid contains the equivalent of 53 kg H_2/m^3, about the same as contained in H_2 compressed to 700 bar. Currently, however, it is mainly used as a preservative, tanning agent for leather, and an anti-icing agent on roads (Acidpedia, no date; NCBI, no date). In terms of its prospects for generating more valuable chemicals via further processing, it essentially represents a thermochemical dead-end.

2.3 Methane and ethylene

Copper (Cu) is the only known metal electrocatalyst capable of forming C_1-C_2 products with appreciable Faradaic efficiencies (Hori, 2008; Kuhl et al., 2012). A typical product distribution is shown in Table 1. Experiments have demonstrated an ability to tune the CH_4/C_2H_4 ratio between ~0.2 and 10 by varying the surface crystal alignment from Cu(111) to Cu(711), with ~50-60% Faradaic efficiency of the main product (Hori et al., 2003). Recently, nanostructured Cu produced by oxidation/reduction cycling and by other means has been shown to increase the Faradaic efficiency of C_{2+} products such as C_2H_4 and ethanol (Ren et al., 2016a, 2016b; Handoko et al., 2016; Dutta et al., 2016; Li and Kanan, 2012). Still, these types of catalysts produce a mixture of reduced species and the required overpotential is quite high, typically –1.0 V.

Table 1. Product distribution for H_2O + CO_2 over a copper catalyst

Product	Faradaic efficiency
Methane (CH_4)	33.3%
Ethylene (C_2H_4)	25.5%
Hydrogen (H_2)	20.5%
Formate ($HCOO^-$)	9.4%
Ethanol (C_2H_5OH)	5.7%
n-Propanol (C_3H_7OH)	3.0%
Propionaldehyde (C_2H_5CHO)	2.3%
Allyl alcohol (C_3H_5OH)	1.4%
Carbon monoxide (CO)	1.3%
Acetaldehyde (CH_3CHO)	1.1%

Source: Hori et al. (1994)

Pure CH_4 could be used as a direct substitute for natural gas, which is primarily composed of CH_4. While natural gas is currently plentiful and inexpensive, it is still a significant contributor to climate change, both through its combustion and inadvertent leaks to the atmosphere (Tollefson, 2013), where its global warming potential is ~30 times that of CO_2 (Myhre et al., 2013). Replacing fossil-derived CH_4 with renewably-generated CH_4 from CO_2RR could be an important long-term energy strategy, as much of the world's energy infrastructure is dependent on this fuel for electricity generation, building heat, industrial processes and, to a more limited extent, transportation (see Section 1).

Ethylene is an important building block for industrial chemical production. More than 50% of the 7.4 EJ/yr of C_2H_4 consumed globally is used to make polyethylene, the world's most widely-used plastic, and it is also used to make precursors to ethylene glycol (anti-freeze), polystyrene, and polyvinyl chloride. As a fuel, it could be used as a blending component in natural gas, directly as a substitute for acetylene in welding, as a non-fermentative route to ethanol (Clark, 2013), or as a precursor to *n*-propanol and propylene (Rodriguez and Tenn, 2012).

2.4 Ethanol and propanol

There are a few reports of the EC formation of ethanol with high Faradaic efficiency (e.g., Ren et al., 2016a). Ethanol could be used with our present infrastructure, as it is already blended with gasoline in numerous countries (Lane, 2016), in addition to being used in higher concentrations in modified engines (e.g., E-85 blends). Techniques for separating ethanol from aqueous electrolyte are, therefore, of interest.

Propanol is also interesting as it can be readily separated from water by liquid-liquid extraction (see Section 3.4.2). Currently, the state-of-the-art catalysts that produce this alcohol achieve about 10% Faradaic efficiency (Ren et al., 2016b).

2.5 Methanol

Methanol would be an attractive product, as it could either be used directly in a methanol economy (Goeppert et al., 2014), or used to make gasoline via the methanol-to-gasoline (MTG) process (NETL, no date; Packer, no date; ExxonMobil, 2008; Helton and Hindman, 2014). It could also be used to make dimethyl ether, which is can be used as a building block for other chemicals (Centi and Perathoner, 2014), as well as a potential substitute for diesel engines and LPG.

Water contamination does not appear to be problematic for the MTG process, as methanol is partially dehydrated to make dimethyl ether and water before reacting to make synthetic gasoline. Moreover, the synthesis process yields more than 50% water by mass, so the process is likely tolerant of small amounts of water in the initial methanol feedstock. While the reaction is exothermic, if too much water is present initially it may affect the reaction temperature, which must be maintained at ≥300°C (Packer, no date).

However, the electrocatalytic pathway that produces methanol is energetically unfavorable compare to that producing CH_4 (Xiao et al., 2016; Xiao et al., 2017). There are experimental efforts underway to realize this reaction, and direct PEC pathways have been explored (Barton et al., 2008), but there is some uncertainty regarding the function of these pathways (Saveant and Tard, 2016). Nevertheless, some recent papers have identified potentially promising pathways (Qiao et al., 2014; Studt et al., 2014; Albo et al., 2015).

2.6 C$_4$ (and higher) hydrocarbons

Centi et al. (2007) and Shibata et al. (2008) have published tantalizing studies indicating that it is possible to produce C_{4+} products electrochemically. Centi et al. in particular even point to aromatics as a specific class of products produced. Shibata et al. report that up to C_6 hydrocarbons can be obtained at room temperature and atmospheric pressure using a commercially available Cu electrode. However, only ~10% of the total products are C_{4+}.

The direct P/EC production of C_{4+} products would be very important, because separation from water becomes easier, and these compounds also become progressively more compatible with existing fuels such as gasoline. However, the large numbers of reducing electrons required to make these products means that they are potentially more challenging to produce at high efficiency than shorter-chain hydrocarbons.

3   Product separation

Because of the number of challenges associated with CO_2RR (low aqueous solubility of CO_2, high numbers of electrons resulting in relatively low efficiency, few catalysts, poor product selectivity, generally high overpotentials, current- or intensity-dependent product distributions, cost and GHG content of CO_2 source; see Section 1.2) due, at least in part, to the early stage of the research, we have deliberately avoided constraining the process options available to realize a viable P/EC CO_2RR system, and our analysis is applicable to chemistries other than ambient temperature and pressure aqueous catholyte-anolyte system designs (e.g., Singh et al., 2015; Singh and Bell, 2016). These include:

- Non-aqueous electrolytes (common laboratory solvents, as well as fluorinated solvents and ionic liquids), offering increased solubility of CO_2 and/or immiscibility of certain products, easing separation
- Gas-phase reactions at the anode, cathode or both
- High pressure or low temperature systems to increase CO_2 solubility, including the possibility of CO_2/water solid clathrates near 0°C (DeCiccio et al., 2015), or the use of supercritical CO_2 (74 bar, 31°C) with a suitable electrolyte
- Elevated temperatures to increase reaction rate, which would be useful in gas-phase systems or non-aqueous solvents with high CO_2 solubility
- Separation of light absorption and electrochemistry (e.g., solar photovoltaic—or even grid electricity—coupled with an EC cell) to create stable cell operation at higher capacity factors and, potentially, current densities
- Separation of CO_2RR into several steps involving fewer electrons each, optimized for different conditions

Given the current heterogeneous catalysts available, all of these options are likely to generate product mixtures that will require post-synthesis separations. In this section, the basic principles of chemical separations using established methodologies are described. Each of these is of potential use for CO_2RR-generated fuels, and the energy required to use them is estimated based on optimum process conditions. Several typical mixtures are used as examples. Many of our examples are for aqueous EC systems (which are the most widely studied), while some come from systems commonly found elsewhere in the chemical industry.

3.1 Theoretical minimum energy required for separations

The energy required for separation of product mixtures is a net loss to the EROEI balance for CO_2RR systems, and is an important consideration for solar P/EC systems. The minimum thermodynamic energy required to reversibly separate mixtures of components is the opposite of the free energy of mixing ΔG_{mix}, which for ideal mixtures is always negative because the enthalpy of mixing ΔH_{mix} is zero:

$$\Delta G_{mix} = \Delta H_{mix} - T\Delta S_{mix} = -T\Delta S_{mix} < 0,$$

where T is absolute temperature and ΔS_{mix} is the entropy of mixing, which for ideal mixtures is:

$$\Delta S_{mix} = -R \bullet \sum x_i \ln(x_i)$$

where R is the universal gas constant (8.3145 J/mol-K) and x_i is the mole fraction of component i. Thus, a 1:1 binary mixture has the maximum entropy of mixing and lowest free energy of mixing (–1.72 kJ/mol at 25 °C). Mixtures of more than two components have more negative free energies.

However, real mixtures can have higher or lower free energies than the ideal case, because of intermolecular forces and non-zero enthalpies of mixing, which can be positive or negative. Across mixtures of water with 16 common liquid solvents plus NaCl, ΔH_{mix} ranges from –0.98 kJ/mol (14 mol% isopropanol) to +1.26 kJ/mol (46 mol% sulfolane). Including entropies of mixing, ΔG_{mix} ranges from –2.43 to +0.24 kJ/mol (–75 to +4 kJ/kg). The ratio of ΔG_{mix} to the enthalpy of combustion (ΔH_c) of the solvent (–4,160 to –470 kJ/mol) can vary from essentially zero to 0.43%. See Section 2 of the Supplementary Information for details.

For multicomponent mixtures, this ratio tends to be larger. Moreover, for lower target product concentrations, this ratio tends to be much higher, scaling roughly inversely with concentration. Because of inefficiencies inherent in non-ideal, real-world processes, separation of mixtures typically requires several times the free energy of mixing, which defines the thermodynamic minimum for reversible separation.

3.2 Phase Separation

Fundamentally, it is much easier to separate substances when they are in different phases (gas-liquid, gas-solid or liquid-solid), though there is typically always a small amount of material in the other phase (e.g., entrained gas in liquid and liquid droplets in gas) that must be removed if high purity is required. Generally speaking, separations that take place over longer times tend to reduce entrainment of the undesired phase, but longer process time can limit the high throughput required for an economically viable system. The use of equipment to promote separation, such as a demister to minimize liquid entrainment in the gas phase, is commonly employed.

When substances occupy the same phase (gas-gas, liquid-liquid or solid-solid), physical or chemical changes are required to effect separation, unless the two (usually liquid) substances are immiscible, in which case gravimetric separation is all that is required. However, virtually all

liquid C_1-C_3 products considered here are miscible with water (and probably each other) under ordinary conditions. While a small number of possible products are solids at or near room temperature (e.g., acetic acid, glyoxal, glycolaldehyde, 1,3,5-trioxane), they are typically not produced at high yield. Moreover, these products would likely dissolve in an aqueous solution, so separation of solids is very unlikely in any realistic CO_2RR system. Nonetheless, we do briefly discuss separation of solids in Section 3.4.4.

3.3 Distillation

Distillation achieves phase separation of two miscible components through temperature and/or pressure modulation. The most common approach is conventional atmospheric pressure distillation, which is widely used in industry.

3.3.1 Conventional distillation, with ethanol/water and petroleum refining as examples

Distillation tends to be inefficient because it requires high heat inputs in the reboiler, while (ideally) rejecting the same amount of heat at lower temperature in the condenser (Kiss et al., 2012). While some of this heat can typically be recovered, Halvorsen and Skogestad (2011) found that the required energy input for conventional distillation can be more than 50% higher than the theoretical thermodynamic minimum, and often much higher. We will not provide a detailed analysis of distillation processes here, as comprehensive references can be found elsewhere (e.g., McCabe et al., 2001; Green et al., 2007), but instead provide perspective on the energetic expense of distillation relative to the energy available from products of P/EC systems. Some of these references include extensive discussion of the design of appropriate distillation systems for numerous separations, which is beyond the scope of this paper.

The fraction, f, of the enthalpy of combustion of the product, $\Delta H_{c,1}$, that is required for separation of the product by distillation, ΔH_d, can be obtained from (based on McCabe et al., 2001):

$$f = \frac{\Delta H_d}{\Delta H_{c,1}} \times 100 = \frac{r\left(¿¿v,1\,\Delta H_{v,1} + x_{v,2}\,\Delta H_{v,2}\right)^x}{\Delta H_{c,1}} \times 100 = ¿$$

where $x_{v,i}$ are the initial vapor-phase mole fractions of the product ($i = 1$) and solvent ($i = 2$) being separated, $\Delta H_{v,i}$ are the corresponding enthalpies of vaporization, and r is the ratio of total moles vaporized to moles of product produced, called the reflux ratio, which can be approximated by $1/x_{v,1}$. Note that the $x_{v,i}$'s will depend not only on temperature but also on the composition of the liquid-phase mixture. The additional enthalpy associated with the sensible heat required to raise each component to the boiling point of the mixture can also be included in this expression, but the enthalpy of vaporization is typically much greater than the enthalpy of sensible heating. It

should be emphasized that, if f is greater than 100%, more energy is used to separate the product than can be recovered by its combustion.

While this calculation provides only an approximation, it is a useful starting point. For a 10 wt% (~4 mol%) ethanol mixture in water with 25 °C initial temperature and 91 °C vaporization temperature, $x_{v,1}$ = 30% (Kosaric et al., 2011). Under these conditions, $\Delta H_{v,1}$ (ethanol) and $\Delta H_{v,2}$ (water) are virtually identical (46 kJ/mol), and $\Delta H_{c,1}$ = 1,220 kJ/mol (NIST, 2017). Therefore, assuming r = 3.3, f is 12.6%, which is close to the result of a more sophisticated model (16%) that obtained 90 wt% ethanol (Kvaalen et al., 1984). For a more dilute initial ethanol concentration (e.g., 1 wt%), the vaporization temperature is 99 °C, $x_{v,1}$ = 2.6% (Kosaric et al., 2011), and f = 146%. (When f is greater than 100%, more energy is used to generate the product than can be recovered by combustion.) This result suggests that distillation is not likely to be a viable candidate separation technique when a dilute target product must be separated from a solvent and/or other products.

Note that ethanol/water and many other systems form azeotropic mixtures, which limit the purity that can be achieved in conventional distillation. The addition of a third component, known as an entraining agent, often makes it possible to achieve higher purities. For example, benzene, cyclohexane, or ethylene glycol is often used with ethanol/water mixtures to produce a nearly 100% water-free ethanol product. However, the addition of an entraining agent typically requires further purification steps to remove it from one or both of the resultant distillation products, further increasing the energetic expense of distillation, though sometimes the entraining agent phase separates from the distillation product(s) upon condensation, making separation and recovery more straightforward (Kosaric et al., 2011).

Another example of azeotropic distillation is the n-butanol/water system, which has a 76 mol% water azeotrope at 92 °C, but produces phase-separated products, with 97% water in the aqueous product phase and 58% n-butanol in the organic product phase (Luyben, 2008). Using a two-column distillation scheme, for a feed concentration of 2 wt% n-butanol in water, 99 wt% n-butanol was obtained with f equal to 25%. This f value is substantially lower than that of ethanol, illustrating that separations from water tend to become more energetically favorable for higher hydrocarbons. Electrochemical conversion of CO_2 to higher hydrocarbons, however, becomes increasingly difficult as more electrons are required to reduce CO_2 to the desired product (see Section 2).

Vacuum distillation is another approach that can be used to circumvent an azeotrope, while also lowering the mixture's boiling point that often results in lower energy inputs compared to atmospheric pressure distillation. For instance, for ethanol/water mixtures, with an atmospheric pressure azeotrope at 95% ethanol by mass, ethanol product purity can be increased to >98% by lowering the pressure to ~0.1 bar (Beebe et al., 1942). By contrast, for systems without an azeotrope such as methanol/water, purities of >99.99% are possible using conventional atmospheric-pressure distillation (Zhang et al., 2010).

The distillation energy used in petroleum refining serves as another useful reference. Using data for the U.S. industry (Morrow et al., 2015), the initial distillation of crude oil into light and heavy fractions yields an f of 3.2% relative to the energy content of the crude oil. Note that this estimate

represents a lower bound on distillation energy consumption because it is part of a highly-integrated plant that utilizes unwanted products and waste heat from other processes to lower overall energy consumption. Including all refinery processes (hydrocracking, etc.) increases f to 9.3%—a better reflection of the total energy required to separate a complex mixture such as crude oil. Note that unlike our above estimate, these metrics are normalized to the total energy of the feed mixture, not just that of the target product. The much lower energy inputs for petroleum refining is a result of much higher product concentrations in the initial crude oil compared with the ethanol examples given above.

While distillation is considered to be mature technology, with >40,000 columns in use in North America consuming ~40% of total energy in the refining and bulk chemical industries (White, 2012), there is nonetheless room for improvement. A number of new approaches have been explored, including dividing wall columns, heat integrated distillation, vapor compression, multi-effect distillation, cyclic distillation, and several types of heat pump schemes; case studies point toward savings of 20-50% over conventional distillation, with potential savings of up to 80% in some cases (Zhang et al., 2010; EPA, 2011; Kiss et al., 2012; Morrow et al., 2015).

3.3.2 Cryogenic distillation, with air separation, C_2H_4/C_2H_6, and CH_4/CO_2 as examples

Cryogenic distillation can be used to separate mixtures of gases with different condensabilities. The most common application is separation of air into nitrogen (N_2), O_2 and argon (Ar). The process requires tight integration between heat exchangers and separation columns to obtain high efficiency. Cooling is accomplished via the Joule-Thomson effect, whereby non-ideal gases typically cool upon expansion (Windmeier and Barron, 2015).[×] Air separation is an example of a three-component separation with close boiling points (all between 77 K and 90 K at atmospheric pressure). A molecular sieve (see Section 3.6.3) is used to remove water, CO_2, and gaseous fuels from compressed air before cryogenic separation (Castle, 2002). The molecular sieve must be regenerated to close the cycle; see Section 3.6.3 for energy requirement estimates.

An example of a two-component cryogenic separation is C_2H_4/C_2H_6. Typically, this separation is done under mild cryogenic temperature conditions (–20 °C) and elevated pressures (~20 bar). To produce pure (99.95%) C_2H_4 from an 80% C_2H_4/20% C_2H_6 mixture requires ~2.7 MJ/kg C_2H_4 (Ploegmakers et al., 2013), or an f of ~5.4%. By comparison, the free energy of mixing of the C_2H_4/C_2H_6 mixture is ~4 kJ/kg (C_2H_4) (Calado et al., 1980), or ~0.16% of the distillation energy.

3.4   Solvent-mediated phase separation

However, all gases exhibit heating at both low and high temperatures, and at all temperatures at sufficiently high pressures. The high-temperature inversion point for most gases is typically several hundred K, but H_2, helium and neon have much lower inversion points, so at room temperature they warm when expanded (Windmeier and Barron, 2015).

3.4.1 Gravimetric separation, with n-*butanol/water as an example*

Gravimetric separation can be accomplished when liquids are immiscible and have different densities. While, as noted earlier, most C_{1-3} liquids are miscible with water, *n*-butanol is immiscible with water above 1.0 M at 20 °C (BASF, 2006). However, ~20 wt% of water remains dissolved in the *n*-butanol phase, and ~8 wt% of *n*-butanol remains in the aqueous phase, requiring further separation. Also, phase separation still requires a finite amount of time to manifest, and in some cases, phases do not cleanly separate, but droplets of one phase remain suspended in the other phase. An example of this issue and its resolution is the salt-induced separation of ethanol from saturated aqueous Cs_2CO_3 solution, discussed in Section 3.4.3 (Singh and Bell, 2016), where a settling tank and coalescer were proposed to convert an ethanol microemulsion into a separate phase with >90 wt% ethanol.

3.4.2 Liquid-liquid extraction, with n-*propanol/water as an example*

An example of liquid-liquid extraction (LLE) is the separation of *n*-propanol from water, which are miscible, via *n*-pentanol as well as longer-chain alcohols (up to *n*-dodecanol; Stoicescu et al., 2011), methyl acetate, ethyl acetate or *n*-propyl acetate (Cehreli et al., 2006). The propanol will preferentially partition into the organic solvent phase, which forms an immiscible layer on top of the water. The propanol must then be separated from its host solvent, but will typically be present in higher concentration, so subsequent separation is more efficient than in the initial mixture.

3.4.3 Salt extraction, with organics in aqueous salt solution as examples

Many liquid fuels can become immiscible in water when salt is added, a process referred to as salt-assisted liquid-liquid extraction (SALLE), or "salting out" (Majors, 2009). Pertinent fuels for which this is applicable are formic acid, acetic acid, ethanol, and several C_3 oxygenates (propionic acid, *n*-propanol and isopropanol) (Merck, 1983; Li et al., 2000; Fu et al., 2015; Singh and Bell, 2016). However, efficient use of materials requires the recovery of the salt; one proposed method uses a saturated Cs_2CO_3 electrolyte that is continuously recirculated after separation of ethanol (Singh and Bell, 2016).

Other products of potential interest, such as acetic acid, acetone, isopropanol and methanol, have been salted out from water in the presence of a third C_{4+} organic-phase solvent such as butanone, cyclohexane or 2-ethylhexanol (Shah and Tiwari, 1981; Hasseine et al., 2009). As noted previously, however, this third solvent must then be separated from the product of interest.

3.4.4 Precipitation of solid CO₂RR products from water

While most C_1-C_3 products are liquids or gases under standard conditions, glycoaldehyde and 1,3,5-trioxane (trimer of formaldehyde) are solids at room temperature. In addition, carboxylic acids such as formic, acetic or proprionic acid are often found in the ionic form (e.g., formate) and can in principle form insoluble salts under some conditions. Moreover, some liquids have freezing points relatively close to that of water (e.g., acetic acid, 16 °C; glyoxal, 15 °C; formic acid, 8 °C; ethylene glycol, -13 °C; proprionic acid, -21 °C; 1,3-propanediol, -27 °C) and could be frozen out of solution, as can water to separate it from other substances. However, the presence of multiple components can have a large influence on the freezing point; for instance, a 40 wt% ethanol solution in water has a freezing point of –23 °C (Engineering Toolbox, no date – a), and forms a solid that is also a mixture of ethanol and water, analogous to the result of distillation.

3.4.5 Estimated energy requirements for solvent-mediated separations of CO_2RR products from water

The energy required to pump fluids is negligible compared with the energy required for distillation or pressurization against a membrane (see Sections 3.3 and 3.5.5). For solvent-mediated phase separation, the main energy input is the embodied energy of the substance(s) inducing the phase separation (solvent and/or salts). The embodied energy of a chemical or object is the cumulative energy input required to produce it in finished form from raw starting materials. Table 2 shows a list of embodied energies for a number of common solvents, fluorinated solvents and ionic liquids, as well as common salts, taken from the Ecoinvent v2.2 database (Ecoinvent, 2012). Note that some items are also reactants or products of CO_2RR, and could be recycled internally or generated by alternative means, potentially lowering the embodied energy. Aside from water, which has a very low embodied energy in most regions (0.006-0.012 MJ/kg), the range of embodied energies for non-fluorinated solvents span 10.9-126 MJ/kg, while the three fluorinated solvents listed are considerably higher (209-217 MJ/kg). Salts, by comparison, have very low embodied energies (3.3-11.1 MJ/kg) unless they contain lithium or fluoride, in which case they are comparable to solvent embodied energies (64-111 MJ/kg).

Table 2. Table of embodied energy of selected solvents (MJ/kg)

Common solvents	
Acetone	57
Acetonitrile	87
Benzene	62
Butanols (average of *n*- and isobutanol)	87
Carbon dioxide (CO_2) (liquid)	10.9
Carbon tetrachloride	35
Cyclohexane	77
Cyclohexanone	108
Dichloromethane	41

Dimethylformamide (DMF)	58
Dimethyl sulfoxide (DMSO)	46
Ethanol	71
Ethyl acetate	65
Hexanes (average of *n*- and isohexane)	64
Isopropanol	63
Methanol	55
Methyl ethyl ketone	54
Monoethanolamine (MEA)	89
Tetrahydrofuran (THF)	126
Toluene	63
Water	0.01
Fluorinated solvents	
Hexafluorethane	209
Tetrafluoroethylene	217
Monochloropentafluoroethane	209
Salts	
Sodium chloride (NaCl)	3.3
Potassium chloride (KCl)	9.0
Calcium chloride (CaCl$_2$)	11.1
Lithium chloride (LiCl)	64
Lithium fluoride (LiF)	111
Ionic liquids	
1-Butyl-3-methylimidazolium tetrafluoroborate ([C$_4$mim][BF$_4$])	124
1-Butyl-3-methylimidazolium bromide ([C$_4$mim][Br])	245

Source: Ecoinvent (2012)

Common ionic liquids in which CO_2 is soluble include the cations 1-alkyl-3-methylimidazolium ([C$_n$mim]$^+$, where C$_n$ = C$_n$H$_{2n+1}$), N-alkylpyridinium ([C$_n$Py]$^+$), or tetraalkylammonium ([N$_{abcd}$]$^+$, where subscripts indicate alkyl chain lengths), coupled to the anions tetrafluoroborate ([BF$_4$]$^-$), hexafluorophosphate ([PF$_6$]$^-$), bis(trifluoromethylsulfonyl)amide ([NTf$_2$]$^-$), halides (particularly [Br]$^-$) (Rees and Compton, 2011), or tetracyanoborate ([B(CN)$_4$]$^-$) (Carvalho et al., 2016). While the embodied energies for most of these ionic liquids are not readily available, two representative compounds ([C$_4$mim][BF$_4$] and [C$_4$mim][Br]) have embodied energies (124-245 MJ/kg) ranging from that of the highest organic solvent to more than those of fluorinated solvents.

By comparison, absolute enthalpies of combustion $|\Delta H_c|$ of C$_1$-C$_3$ products (aside from CO and formic acid, both of which are ≤10 MJ/kg) range from 14.6 MJ/kg (acetic acid) to 55.5 MJ/kg (CH$_4$). If solvents (and to a lesser extent, salts) are not recycled and are used in quantities comparable to the amounts of products produced, the invested energy could easily exceed that yielded by the products. Therefore, it is imperative that these substances be recycled with high

efficiency in order to keep the invested energy per product combustion enthalpy small. The energy lost in unrecovered solvents and/or salts can exceed that of distillation, unless recovery is very tightly controlled. As an example, for isopropanol with $|\Delta H_c|$ = 33.4 MJ/kg, the energy loss (as a fraction f of isopropanol's combustion enthalpy) associated with 1% solvent mass lost per mass of isopropanol could be as low as 0.3% (or less) for common salts, or as much as ~7% for compounds with high embodied energies such as fluorinated solvents or ionic liquids, e.g., comparable to distillation. However, the actual energy penalty is probably higher, at least at the low end of this range, because the separation energy cannot be lower than the theoretical minimum, which for simple binary mixtures we determined in Section 3.1, could have an f as high as ~0.4%.

3.5   Membrane separation

Membranes are currently employed in several high-volume industrial separations, including enrichment of O_2 or N_2 from air, removal of CO_2 from natural gas (CO_2/CH_4) or industrial flue gas (CO_2/N_2), H_2 recovery from petrochemical streams (H_2/N_2, H_2/CH_4, H_2/CO), and separation of volatile organics from water or water vapor (Yampolskii, 2012). Furthermore, several high value separations, such as olefin/paraffin separation (ethylene/ethane and propylene/propane), are the target of current membrane development, as membrane-based processes would likely be much less energy intensive than traditional separation technologies (Sanders et al 2013). Here, we briefly review some of these key separations for several reasons: 1) to provide illustrative examples of the energy savings that can be realized by membranes relative to conventional technologies, 2) to describe the challenges that remain in the deployment of membranes at large scale, and 3) to suggest that membrane separations could be useful for CO_2RR products, since many of the chemical species relevant to industrial membrane separations also appear as products or reactants of CO_2RR (e.g., CO_2, CO, CH_4, ethylene, methanol, ethanol, etc.)

Membranes are thin barriers that selectively permit the passage of one or more chemical species while rejecting the passage of other species. Most commonly, membranes are comprised of organic polymeric materials, which are generally mechanically robust and inexpensive. Other materials, such as ceramics, metals, and supported liquid films, are employed in special applications, but these materials are often more expensive than polymeric membranes and, in the case of ceramics and liquid films, lack mechanical resilience (Baker 2012). Hybrid materials, which are composites of polymers and inorganic adjuncts, can have good stability, separation, and mechanical characteristics, but are at an early stage in their development (Bachmann et al. 2016). Because a phase change is not required to effect separation (with the exception of pervaporation applications, discussed in Section 3.5.4), membrane systems are generally energy efficient (Kamcev et al. 2016) compared to, for example, distillation systems. The separatory layer of a polymeric membrane is generally very thin (~100 nm), but is supported by a much thicker (~100 µm) high-permeability layer for mechanical resilience. For more information, see Section 3 of the Supplementary Information.

3.5.1   Separation of air

Although not directly relevant to separation of CO_2RR products, enrichment of N_2 from air is one of the largest industrial membrane applications, so is worth summarizing briefly. Air separation has been conventionally accomplished by cryogenic distillation (Section 3.3.2) or pressure swing adsorption (PSA) (Section 3.6.4), which are typically used to produce N_2 at high flowrates and purities exceeding 95%. N_2 is used in refrigeration, blanketing, and ammonia synthesis, among other applications. Polysulfone [a type of poly(diphenyl ether)] is a chemically, thermally, and mechanically resilient industrial thermoplastic that is the dominant membrane material used for air (and H_2) separations (Sanders et al. 2013). Membrane systems, which operate with feed pressures of approximately 8-10 bar (Baker 2002), are the most economical option for N_2 at low flowrates (~6 to 1,200 m^3/h). While membranes are capable of producing N_2 with purities up to 99%, the selectivity/permeability tradeoff dictates that membrane productivity at such high product purity is low. Membranes that produce N_2 at 95% purity typically operate at recoveries of 50%, but the N_2 recovery drops to about 25% for membranes capable of producing N_2 at 99% purity (Baker 2002). (Recovery is the ratio of product to feed stream flowrates.)

3.5.2 Separation of CO_2 from gas streams

Membrane systems currently compete with amine adsorption technologies for removal of CO_2 from various gas streams, including industrial flue gas, natural gas, and various other products during enhanced oil recovery (Sanders et al. 2013, Spillman 1989). These streams are complex mixtures, with composition varying with location and time. While the development of membranes capable of removing CO_2 from various mixtures has been motivated largely by pipeline specifications limiting CO_2 and H_2S concentrations in natural gas, membranes could potentially also be used to concentrate CO_2 as a feedstock for a solar fuels generator or remove leftover CO_2 from the CO_2RR product stream. Cellulose acetate membranes dominate in CO_2/CH_4 (natural gas) separation applications despite the relatively low permeability of cellulose acetate to CO_2 (4.8 Barrer[i] to pure CO_2). Cellulose, the precursor to cellulose acetate, is an abundant raw material, so cellulose acetate membranes are relatively low cost and large membrane areas may be used to compensate for low permeability without incurring extraordinary capital expense. Many other materials have been tested for CO_2/CH_4 separation, but no other suitable membranes have been found that can perform a satisfactory separation at the feed conditions (approximately 50 °C and 65 bar). Plasticization by CO_2, which tends to increase diffusivity of all species and thus decrease product selectivity, is the most frequently encountered challenge in this application (Baker and Low 2014).

3.5.3 Separation of hydrocarbons, with C_2H_4/C_2H_6 and C_3H_6/C_3H_8 as examples

The separation of unsaturated from saturated hydrocarbons (olefins and paraffins, respectively), conventionally performed using cryogenic distillation at elevated pressure (Eldridge 1991, also see Section 3.3.2), is energy intensive, and is an ongoing target application for membrane development. C_2H_4 and C_3H_6 are the largest volume chemical feedstocks for the petrochemical industry (see Figure 2), and they are obtained from petroleum refining as a mixture with light

i One Barrer is approximately equal to $3.34×10^{-16}$ mol Pa^{-1} s^{-1} m^{-1}.

paraffins (Eldridge 1991). Ethylene is also a commonly-reported product of CO_2 reduction (see Section 2.3). The separation trains required for C_2H_4/C_2H_6 separation, for example, can cost over a billion dollars each, and the total distillation energy consumed by olefin/paraffin separations in the U.S. was 130 PJ in 2009 (Sanders et al. 2013), or $f = \sim7\%$ (combined enthalpies of combustion of C_2H_4 and C_3H_6). Membrane separation could substantially reduce the energy requirements for these separations, but current membrane materials do not exhibit adequate selectivity. Traditional membrane materials generally have C_3H_6/C_3H_8 selectivities <5. Emerging polyimide materials have exhibited selectivities in the range of 10-15 at 35 °C, but these materials also have very low permeabilities (typically <1 Barrer) (Burns and Koros, 2003; Das and Koros, 2010). Permeabilities tend to be higher for C_2H_4/C_2H_6 mixtures (1-2 Barrer), but selectivity for this separation is poor (typically 3-5) (Staudt-Bickel and Koros 2000).

Like CO_2 separations, a significant challenge in developing membranes for olefin/paraffin separations is membrane plasticization, which tends to be severe with these highly condensable solutes (Sanders et al. 2013). Therefore, continued development of membranes with improved selectivity and stability is needed. Even if membranes do not have the required selectivity and permeability to perform the desired separation in a single pass, multiple-pass systems or hybrid membrane-distillation systems could operate with substantially lower energy inputs than conventional cryogenic distillation columns (Sanders et al. 2013).

3.5.4 Pervaporation to remove organic CO_2RR products from water

Pervaporation combines aspects of membrane separation and distillation, and has been deployed on large scale in two primary applications: the dehydration of concentrated alcohol solutions, and the removal of small amounts of volatile organics from water (Baker 2012). Both of these systems have direct relevance to CO_2RR product separation. In particular, pervaporation is useful in separating azeotropic or close-boiling mixtures that would otherwise be challenging to distill by conventional means (Meier-Haack et al. 2001). The feed mixture contacts the membrane as a liquid, and the permeate side of the membrane is typically held under reduced pressure such that any solutes that pass through the membrane evaporate from the membrane surface. Permeate is recovered in liquid form using a condenser (Sanders et al. 2013). The quality of the separation is a function of the relative volatility of the components in the feed, the membrane selectivity, and the operating conditions, such as temperature. In a typical alcohol dehydration application, the water content of an ethanol feed can be reduced from 10 wt% to less than 1 wt%, avoiding the challenges associated with distillation of an azeotropic solution (Baker 2012, Martin et al. 1998).

Membrane stability is a significant concern in pervaporation applications. To encourage the separation of volatile components, pervaporation systems are often operated at elevated temperatures, where alcohol/water mixtures can contribute to membrane degradation. The removal of small amounts of volatile organics from aqueous solution (rather than small amounts of water from alcohols) has also been demonstrated using pervaporation (Blume et al. 1990). Generally, the optimal concentration of organic compounds in the aqueous feed is up to ~5 wt%. Batch pervaporation systems are able to remove at least 99% of the volatile organics from such streams.

Most current pervaporation systems are small compared to industrial distillation systems (typically less than 5000 L/h of alcohol solution). In these small plants, the membrane cost can be 15-40% of the total plant cost. Energetically, pervaporation requires ~700 kJ/kg of ethanol, or f = ~2.4%, whereas azeotropic distillation requires roughly six times this amount (Baker 2012). However, conventional distillation scales more favorably than pervaporation systems as feed volumes increase. Current membranes do not have the required selectivity, permeability, or stability to compete with large-scale distillation systems, but the development of improved membranes, as well as improved heat/energy management techniques that would permit superior process intensification, could allow pervaporation systems to capture a larger market share (Baker 2012).

3.5.5   Estimated energy inputs for membrane separations

The flux of solutes through a membrane is driven by a gradient in chemical potential over the membrane, which is typically manifested as a pressure differential. The energy required to pressurize gases can be calculated from simple thermodynamics. Assuming isothermal compression, the energy required to pressurize gases is $nRT\ln(P_2/P_1)$, where n is the number of moles of gas, R is the universal gas constant, T is absolute temperature, and P_1 and P_2 are the initial and final pressures. Typically, membranes are pressurized to several times atmospheric pressure. For a tenfold pressure increase (e.g., from 1 to 10 bar) at 300 K, the required energy is 5.7 kJ/mol (356 kJ/kg for CH_4, or f = ~0.6%), though actual compressors are less efficient than this, ranging from ~65-90% depending on type (Moshfeghian, 2015). Thus, for pressurization of a 50 mol% CH_4 mixture requires an f of ~1.4-2.0%, whereas a 10 mol% CH_4 mixture would require five times this ratio.

For incompressible liquids, the pressurization energy is much less than for gases, and is given by the ratio of the pressure difference to density (Engineering Toolbox, no date – b). For instance, to pressurize water (with density 1,000 kg/m^3) from 1 to 10 bars requires only ~16 J/mol (~900 J/kg), about the same energy as a hydrostatic head of 100 m.

To estimate the embodied energy of membranes, we examined a wide range of polymers (94 in all) in the Ecoinvent database, ranging from 30 to 236 MJ/kg (Ecoinvent, 2012). Perfluorocarbon polymers have energies greater than 200 MJ/kg, and polysulfones used in air separation have embodied energies of ~220 MJ/kg. Other polymers have a maximum embodied energy of 148 MJ/kg. Cellulose acetate polymers used in CO_2 separation have embodied energies of 99 MJ/kg, whereas polyamides (nylons), membrane materials commonly employed in reverse osmosis water purification and gas separations, have embodied energies of 122-137 MJ/kg (when glass fiber composites, irrelevant for membranes, were excluded). See Figure 3.
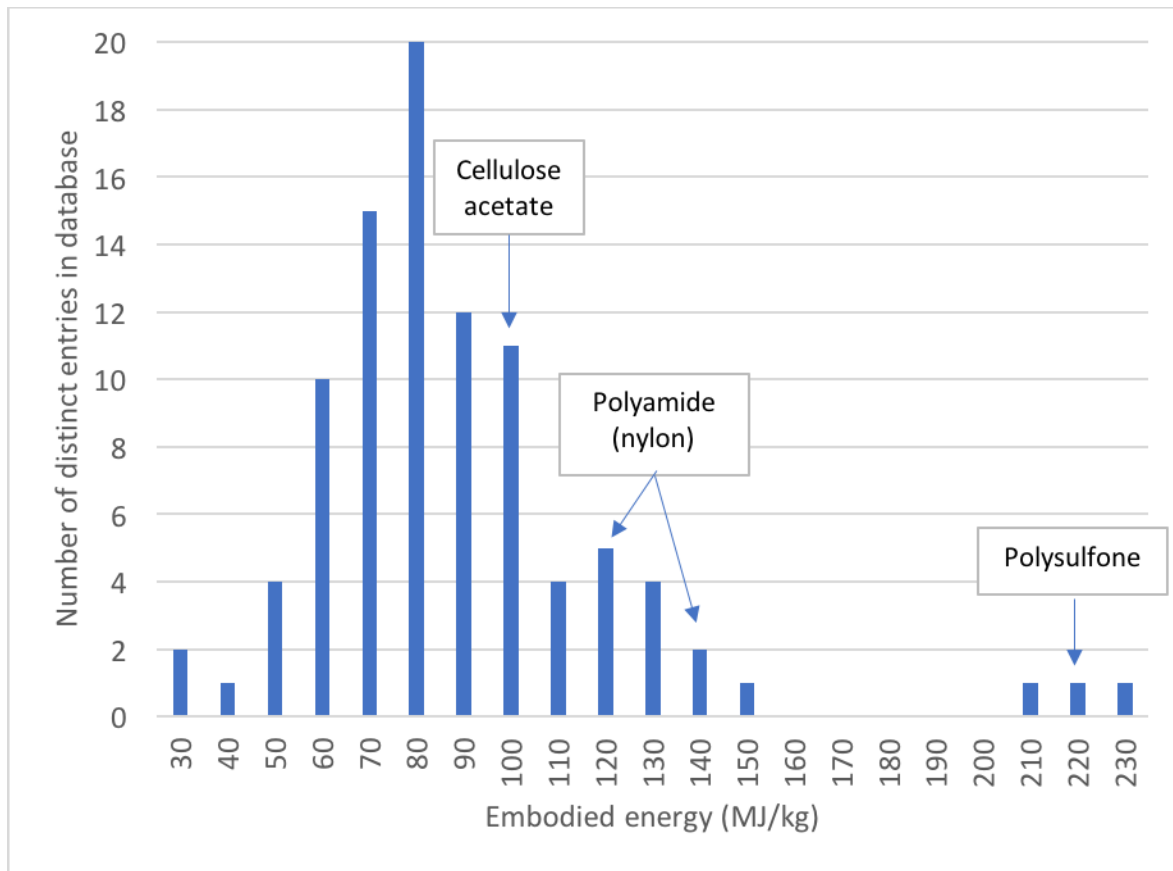
Figure 3. Embodied energy of various polymers. Common polymers used in membrane separations are indicated.

For all these membranes, the "active" (separatory) layer tends to be extremely thin (~100 nm) while the support layer is much thicker (~100 µm) (Baker 2012). This support layer can be made from the same material as the active layer, with the pore size varying across the membrane width, or a separate material (usually polysulfone) with high permeability used as a support layer. Regardless of the active layer material used, the support layer will dominate the total embodied energy.

As for solvent or salt-based extraction techniques, the amount of membrane material consumed per product separated is a key metric. However, it is important to consider that a membrane with a lifetime of 3-5 years contributes negligibly to the overall energy invested in a separation system: assuming polysulfone with an area of 3,600 m^2 is required to produce 1,000 m^3/hr of gas (11.4 mol/s),[x] a total thickness of 100 µm and density of 1,240 kg/m^3 (IDEX, 2017) requires ~450 kg of material. With an embodied energy of 220 MJ/kg and lifetime of 3 years, the membrane embodied energy flow is ~33 GJ/yr. Assuming gas separation is CH_4 with combustion enthalpy of 890 kJ/mol and 90% capacity factor, this system produces ~320,000 GJ/yr of CH_4. Therefore, the embodied energy of the membrane polymer is negligible (f = ~0.01%) compared with the combustion enthalpy of produced CH_4.

Here we assume permeability of 1 Barrer, pressure difference of 1 MPa, temperature of 298 K, and active material thickness of 100 nm.

3.6 Reversible reactions to separate mixtures

In this section, we briefly discuss reversible physical or chemical bonding approaches to chemical separations.

3.6.1 Differential solubility to separate gas mixtures

Various approaches exist to change the concentrations of product mixtures using differential solubility. This technique typically takes advantage of the differing solubilities of gaseous products to preferentially partition them into a liquid solvent. An example is the use of water to separate CO_2 and CH_4 in biogas. Known as "water scrubbing," the higher solubility of CO_2 relative to CH_4 allows it to preferentially dissolve in water, effecting separation. The required energy input needed to produce 98 wt% CH_4 from biogas (containing ~50% CH_4 and ~50% CO_2) in a 10 bar pilot-scale plant has f = ~5% (Nock et al., 2014). Similarly, poly(ethylene glycol) has been used to remove CO_2 from biogas, and is estimated to require f = 7-9% to regenerate (Luostarinen et al., 2011).

3.6.2 Temperature-swing adsorption for CO_2 separations

An example of temperature-swing adsorption is the use of monoethanolamine (MEA) to remove CO_2 (and H_2S) from combustion gases. MEA has been proposed for large-scale CO_2 capture from power plants. The energy required to liberate captured CO_2 from MEA is ~4.0 MJ/kg at large scale (Kothandara, 2010; Luis, 2016). While a number of alternatives (e.g., ammonia, other amines, N-containing amino acids, potassium or sodium carbonate, ionic liquids) have been proposed with regeneration energies as low as ~30% that of MEA, most have drawbacks in terms of physical size of the absorber unit, cost, component corrosion, or solvent degradation that make MEA difficult to improve upon. Assuming a gas stream of 90 wt% CH_4 in CO_2, the regeneration energy has f = 0.8%, while at lower concentration (e.g., 50 wt% CH_4 in CO_2) this energy is a much higher fraction (f = ~7%).

While degradation of MEA is a concern [losses of ~0.2%/hr (Supap et al., 2009) or 0.3-0.7 kg per ton of CO_2 removed (Kothandara, 2010) have been reported], with experiments observing loss rates of ~0.2%/hr (Supap et al., 2009) or 0.3-0.7 kg per t CO_2 removed (Kothandara, 2010), the net energy penalty from such losses are negligible. With an embodied energy of 89 MJ/kg for MEA (Ecoinvent, 2012) and assuming a 90% CH_4/10% CO_2 mixture, we estimate that the additional energy loss is ~3-7 kJ/kg CH_4, or $f \lesssim 0.01\%$. Thus, energy inputs are dominated by MEA regeneration.

3.6.3 Molecular sieves, reversible reagents, and biomaterials

Molecular sieves (high surface-area molecular "sponges," or zeolites) are often used to adsorb water, CO_2, and fuel molecules of various lengths depending on pore size. The captured

substances are subsequently released through heating to ~175-315 °C, with recharge energy (Sigma-Aldrich, 2017) estimated at ~6.0 MJ/kg water removed, assuming 70% heating efficiency. Thus, a product such as ethanol, with 5 wt% water, will require f = ~1.0% to remove adsorbed water, but at higher fractions of water (e.g., 50 wt%), a much larger f (~20%) would be required.

Hygroscopic inorganic salts such as calcium chloride, or sodium, magnesium or calcium sulfate can also be used to remove water from many organic solvents, and can be easily regenerated with heating; for instance, sodium sulfate requires only 25 °C for full regeneration. Reactive drying agents such as calcium hydride or lithium aluminum hydride are also very effective (Bacher, 2016), but are not designed to be easily regenerated.

Copper oxide and palladium are effective regenerative catalysts for removing O_2 and other reactive gases (CO, H_2) from gas streams (*e.g.,* BASF, no date). Nickel is especially reactive with CO, forming liquid nickel carbonyl under standard conditions that is reversible with heating to 150 °C (Roberts-Austen, 1898); this process was the leading industrial technology for producing pure nickel in the 19th century. Other metal catalysts, such as bare copper, or oxides of copper, aluminum or zinc, are used to convert reactive species such as allyl alcohol into oxidation products (CO, CO_2, water) as well as other fuels (propanal, acrolein) (Weston and Adkins, 1929; Schulz and Cox, 1993).

Various kinds of biomaterials, such as sawdust, cornmeal or tapioca pearls can also be used as drying agents. Like most other materials, they can be regenerated via heating, though eventually they become less effective and must be discarded (Wallheimer, 2011). As biomaterials, however, they will decompose naturally and so present less of a disposal burden than inorganic materials (and if grown without appreciable fossil fuel inputs or disturbances of land carbon stocks, their net GHG emissions can in principle remain low).

3.6.4 Pressure-swing adsorption to separate gases from CO_2RR products

Pressure-swing adsorption (PSA) provides another mechanism for separating gases without requiring temperatures far beyond ambient. Typically, a zeolite is exposed to inlet gas at high pressure, forming an adsorbed layer of the desired gas. Upon reduction of pressure, the gas is liberated. The size of the compressor, and hence energy use, is much reduced over that of a liquefaction plant. As an example, PSA competes commercially with cryogenic distillation for the separation of O_2 from air at lower production volumes (≤100 t/day) (Chong et al., 2016). Vacuum PSA is similar to PSA, but at reduced pressure. The use of PSA to remove CO_2 from biogas requires f = 15%, where the input energy is the primary energy needed to produce electricity for compression (Luostarinen et al., 2011).

3.7 Required separation energy

Table 3 summarizes our estimates of the energy required for product separations discussed in this Section. Since a large range of products and concentrations are covered, these estimates are

necessarily approximate, but they nonetheless provide an overall view of what is required for the specific case of CO_2RR product separations. Roughly speaking, distillation and its variants are the most energy-intensive separation approaches, typically requiring an f of ~10% when products are fairly concentrated ($\geq$10 wt%), and much more energy when products are dilute. This result suggests that distillation is not likely to be a viable candidate separation technique when a product must be separated from a significant volume of solvent or carrier gas. By contrast, solvent-mediated separation approaches can have lower energy requirements, provided that solvent loss rates are low (~1% per mass of product produced). Membrane-based approaches and reversible reactions can also drive lower energy separations. However, for all separation methods, energy requirements will vary with the target product, initial concentration, other input stream components, specific approach used, and efficacy of implementation.

Table 3. Summary of estimated energy inputs required for product separation via different approaches

				Separation energy	
Separation method	**Approach**	**Target product**	**Input stream (wt%)**	**MJ/kg of product**	**f (ratio to enthalpy of combustion)**
Thermodynamic minimum	Derived from enthalpies and entropies of mixing	16 common solvents plus NaCl[a]	1.4% to 98.5% in water	~0 to 0.075	~0% to 0.43%
Induced phase change (distillation[b])	Conventional distillation	Ethanol	10% in water	4.7	16%
			2% in water	22	73%
			1% in water	45	150%
		All refined products	Crude oil	2.0 5.8	3.2% (distillation only) 9.3% (complete separation)
	Cryogenic distillation	C_2H_4	80% in C_2H_6	2.7	5.4%
		CH_4	50% in CO_2	5.3 to 6.7	9.5 to 12%
		Olefins (C_2H_4/C_3H_6)	Olefin/paraffin mixtures	3.6	7.3%
	Conventional distillation with heterogenous azeotrope	n-Butanol	2% in water	9.0	25%
Solvent-mediated phase separation[c]	Conventional organic solvent (e.g., hexanes)	Isopropanol	50% in water	0.64	1.9%
	Fluorinated solvents			~2.1	~6.3%
	Ionic liquids			1.3 to 2.5	3.7% to 7.3%

	Common salts			<0.1	<0.3%
	Lithium fluoride			1.1	3.3%
Membrane separation	Pervaporation	Ethanol	50% ethanol in water	~0.7	~2.4%
	Pressurization of gases from 1 to 10 bars (pressurization of liquids is lower)	CH_4	50% in unwanted gas	~0.8 to ~1.1	~1.4% to ~2.0%
			10% in unwanted gas	~4.0 to ~5.5	~7% to ~10%
	Membrane replacement		50% in unwanted gas	~0.006	~0.01%
Reversible reactions	Water scrubbing	CH_4	50% in CO_2	~3	~5%
	Polyethylene glycol			4 to 5	7% to 9%
	Temperature-swing adsorption with monoethanolamine			4.0	7.2%
			90% in CO_2	0.4	0.8%
	Monoethanolamine solvent loss			~0.003 to ~0.007	~0.005% to ~0.013%
	Molecular sieve	Ethanol	95% in water	~0.30	~1.0%
			50% in water	~6.0	~20%
	Pressure-swing adsorption	CH_4	50% in CO_2	8.3	15%

Note: For all methods, required energy input approximately scales inversely with target product concentration. [a] See Supplementary Information, Table S3 for more information. [b] Integrated approaches can confer a 20-50% improvement over standard distillation (see Section 3.3.1). [c] Assume 1% solvent mass lost per mass of product (energy scales linearly with solvent loss rate).

All separations require greater energy investment when product concentrations are low, with energy scaling approximately inversely with initial product concentration. For dilute solutions of ethanol in water, for example, the energy investment for distillation can exceed the product enthalpy of combustion for concentrations of less than 2 wt%, so less energy-intensive approaches are more likely to be successful.

3.8 Degree of separation

Separating relatively pure products produced by P/EC CO_2RR has a number of challenges. Product mixtures with advantageous chemical or physical properties (e.g., multiple phases, differing solubilities, etc.) will be easier to separate, but will likely require energy inputs somewhere in the process, such as replacing solvent lost during extraction (see Section 3.4) or regeneration of dessicant material (see Section 3.6.3). Dilution of the target product with unreacted feed material, co-products or inert compounds will contribute to increased separation energy requirements. While theoretical minimum energies are indeed small, separation technologies typically operate far from these values, with distillation perhaps serving as an extreme example: for a dilute target product requiring energy inputs comparable to its

combustion enthalpy, the required energy could be several thousand times the thermodynamic minimum. Solvent-mediated and membrane-based methods offer lower-energy separation solutions, but these are neither universally available nor are they always cost-competitive with distillation, which typically offers high product purity and high throughput.

One way to circumvent this seemingly intractable situation is to find ways to use product mixtures "as is," with examples given such as CH_4/C_2H_4 mixtures with H_2, CO_2 and other impurities; ethanol/methanol mixtures; or methanol/water mixtures as inputs to the MTG process. However, the utilization of fuel mixtures would not be trivial, given the often exacting design specifications of current combustion devices as well as the associated infrastructure needed to transport, store and dispense the fuels. An example of the requirements for implementing this approach for CH_4 mixtures is explored in detail in Section 5.

4   Separation flow: an example for products from electrochemical CO_2RR by a copper catalyst

In this section, we consider separation of a complex mixture of CO_2RR products as measured by Hori et al. (1994) arising from EC reaction of CO_2 and water on Cu shown in Table 1 and Figure 4. These products are grouped as follows:

- Gases: CH_4, C_2H_4, H_2, CO, and acetaldehyde; CO_2 and water vapor (unused reactants); as well as any carrier gases (N_2, Ar, etc.). While most O_2 product would remain on the anode side, some leakage to the cathode side is inevitable, so O_2 would also have to be removed.
- Liquids: Formate, ethanol, propanol, propanal, and allyl alcohol; water (unused reactant), other solvents (in non-aqueous system), and dissolved electrolyte salts.

Figure 4 illustrates the following hypothetical separation steps:

First, gases and liquids are separated by dissimilar phases. If necessary, a degasser can be used to purge the liquid stream of dissolved gases, and a coalescer used to remove condensable vapors from the gas stream (see Section 3.2).

After water removal with a regenerative dessicant, the gas mixture can be used directly (pathway (**a**); see Section 5) or separated using a variety of methods. Condensation and removal of acetaldehyde by cooling gases to <20 °C would likely be performed first.

Pathway (**b**) involves liquefaction of C_2H_4 and CO_2, which can occur at or near room temperature at elevated pressure (~50 and ~70 bar, respectively), allowing facile separation from other gases. However, such separations likely will not result in pure products, and further processing is necessary to achieve high purity. Gases such as CO and O_2 are fairly reactive, and if not needed, could be selectively removed with regenerative reagents such as copper oxide or nickel (see Section 3.6.3). The water-gas shift reaction could also be used to convert CO to H_2 (which also consumes some H_2O and produces additional CO_2) (Newsome, 1980).

Pathway (**c**) offers an alternative route (useful when pressurization is unable to remove all product gases): sequential membrane separation of C_2H_4, CH_4 and H_2, leaving N_2, Ar and other gases. Membrane separation is discussed extensively in Section 3.5.

Pathway (**d**), staged cryogenic distillation, is more energy intensive but can cleanly separate all the product gases. Distillation is discussed in Section 3.3.

On the liquid product side, reactive allyl alcohol can be selectively removed with a metal catalyst (see Section 3.6.3), producing gaseous (CO, CO_2) and liquid (propanal, acrolein, water) products. Gases will phase separate from solution, though the new liquid products would have to be subsequently separated. Remaining liquids will be a mixture of ethanol, *n*-propanol, water and/or other solvent(s).

Pathway (**e**) provides separation via staged distillation, after using a regenerative dessicant to remove water. Pervaporation, combining distillation with membrane separation, may also be possible; see Section 3.5.4.

Pathway (**f**) is another option available for some alcohols. Ethanol might be removed with a saturated Cs_2CO_3 solution as explored in Singh and Bell (2016), whereas *n*-propanol (as well as isopropanol) can be separated via liquid-liquid extraction (LLE) or salted out using NaCl. Both of these techniques are discussed in Section 3.4. While these alcohols would be the major products of interest, the remaining liquids—a mixture of formate, propanal, acrolein and water— could be combusted for heat or electricity, discarded, or subsequently separated.
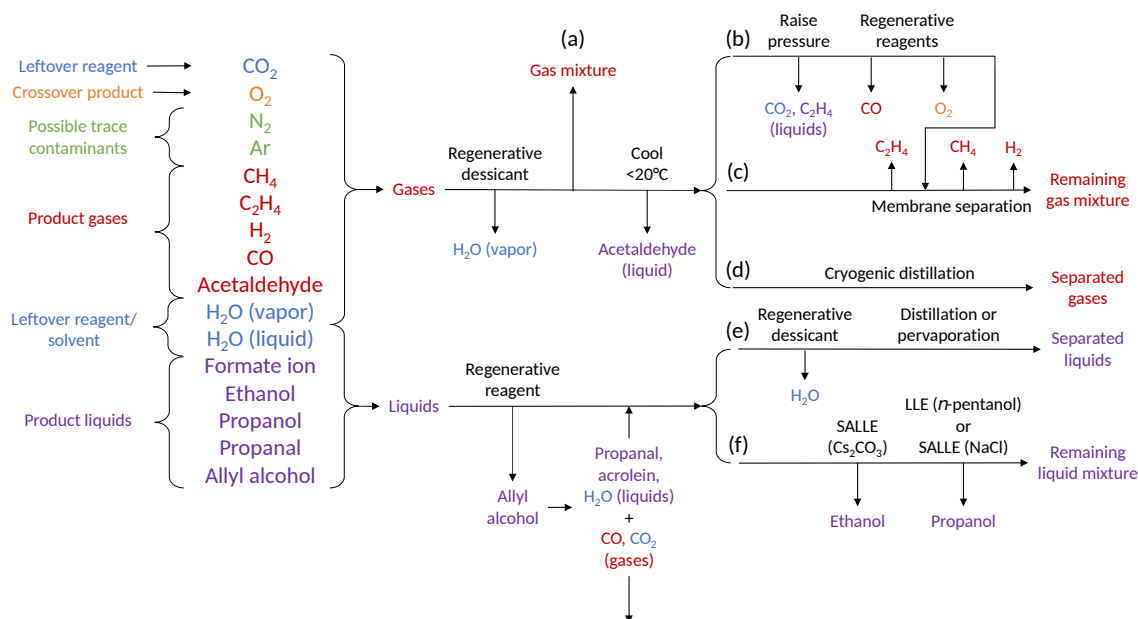

Figure 4. Possible separation approach for mixture of CO_2RR products, reagents and contaminants. In addition to what is shown in diagram, small amounts of liquids will be present in their vapor phases, and small amounts of gases will be dissolved in the liquids, and will have to be removed as well. Abbreviations: argon (Ar), carbon dioxide (CO_2), carbon monoxide (CO), ethylene (C_2H_4), hydrogen (H_2), methane (CH_4), nitrogen (N_2), oxygen (O_2), water (H_2O).

5 Opportunities to minimize separations: use of gas mixtures from CO_2RR using a copper catalyst

As noted in Section 1, there are important tradeoffs among P/EC CO_2RR catalyst capability, product separation efficiency, and compatibility with current fuel (and chemical) infrastructure. Progress in any one of these areas, such as the efficient production of methanol, could open up many new possibilities. By identifying the limitations of catalysis and separation, attention can be focused on the important basic science research that could advance overall progress. Moreover, dialog between the solar fuels community and product end users or regulators (e.g., petrochemical, biofuel and basic chemical industries, vehicle and equipment manufacturers, and climate and energy policymakers) will also become essential.

In this section, we consider the case of using a mixture of several CO_2RR products produced from Cu catalysis directly as a natural gas substitute. While natural gas is not the only application of such an approach, it may represent a near-term opportunity due to the widespread use of natural gas as a convenient and inexpensive energy carrier that nonetheless has appreciable GHG emissions when burned.

Natural gas is mainly composed of CH_4. In the ideal case, a P/EC system would produce nearly pure CH_4 with minimal separation required, and the resulting product would be injected directly into the existing natural gas pipeline system. However, it is not yet known how to produce pure CH_4 via P/EC CO_2RR, so instead we explored whether the mixture of products produced via reaction on Cu, producing CH_4, C_2H_4, H_2, CO and other gases could be used more or less directly in natural gas pipelines, subject to certain constraints.

U.S. natural gas pipeline specifications limit inert gases to ≤4% (primarily CO_2 and N_2), and a gross heating value of 950-1,150 Btu/scf (837-1,013 kJ/mol). CH_4 has a combustion enthalpy of 1,011 Btu/scf, whereas C_2H_4 is 1,602 Btu/scf and H_2 and CO are both ~320 Btu/scf (most other species produced from Cu in small quantities, including acetaldehyde, ethanol, propionaldehyde, allyl alcohol, and propanol, have heating values >1,150 Btu/scf). Therefore, pure CH_4 is acceptable, but too much of these other constituents can push the mixture outside the required specifications. Also, almost all water must also be removed to prevent condensation/freezing in pipelines and equipment corrosion.

Natural gas blending rules also limit the amount of H_2 in pipelines in order to minimize H_2 leaks and metal embrittlement, although compositional tolerances are unclear. Various studies indicate different maximum blending levels (Altfeld and Pinchbeck, 2013; Melaina et al., 2013; Hodges et al., 2015); the overall conclusion is that the safe level for H_2 blended into natural gas pipelines is ≤20%, and must be assessed on a case-by-case basis due to differences in pipeline materials, operating pressures, and states of repair. Other impurities that must be completely removed from natural gas (e.g., H_2S, Hg, oils) and/or biogas (amine, chlorine and siloxane compounds) (Luostarinen et al., 2011; Götz et al., 2016; Corvini et al., no date) are not produced from CO_2RR so would not be problematic unless contamination or degradation of materials occurred.

As a poisonous gas, CO concentration in natural gas must also be kept extremely low to limit public exposure from inadvertent leaks. The EPA (2016a) sets a safe limit for ambient CO

concentration at 9 ppm (8-hr. average), and 35 ppm for acute (1-hr.) exposure. To estimate the maximum permissible CO level in natural gas, we also considered exposure limits for CH_4, its main constituent. The U.S. workplace exposure limit for CH_4 is 1,000 ppm (8-hr. average), and CH_4 poses an explosion risk at lower concentration (5%) than it would pose as a simple asphyxiant (AET, 2010; CDC/NIOSH, 2014). We use this latter threshold in combination with the acute CO exposure limit of 35 ppm to provide a maximum CO concentration in pipeline gas of 700 ppm.

Based on the results from Hori et al. (1994, 2003) with different ratios of C_2H_4/CH_4 and assuming that most CO_2, H_2O, O_2 and liquids were previously separated, other components will include H_2 and small amounts of CO, acetaldehyde, ethanol, proprionaldehyde and other combustibles in the gas phase. We examined six cases varying by C_2H_4/CH_4 product ratio; see Table 4. In all cases, CO concentrations were many times our estimated safe level; therefore, CO levels must be reduced to almost zero. The water-gas shift reaction (Newsome, 1980) could be used by adding sufficient water (before dehydration) to convert CO to CO_2 and H_2; this conversion was reflected in the table of values.

Table 4. Product distributions from Cu catalyst CO_2RR reactions

	Case number					
	1	**2**	**3**	**4**	**5**	**6**
Catalyst	Cu	Cu(100)	Cu(711)	Cu(511)	Cu(311)	Cu(111)
Molar fraction of initial product stream						
Methane (CH_4)	23.2%	32.2%	4.4%	9.1%	29.9%	31.3%
Ethylene (C_2H_4)	11.8%	28.6%	29.6%	20.9%	13.2%	3.7%
Hydrogen (H_2)	57.1%	28.8%	55.5%	58.1%	44.2%	44.0%
Carbon monoxide (CO)	3.6%	3.8%	3.9%	6.1%	8.6%	17.3%
Acetaldehyde (CH_3CHO)	0.6%	1.4%	0.9%	0.9%	0.7%	1.1%
Ethanol (C_2H_5OH)[a]	0.6%	1.6%	1.0%	1.5%	0.4%	0.3%
Propionaldehyde (C_2H_5CHO)[a]	0.7%	1.3%	2.1%	1.1%	0.9%	0.2%
Other combustible gases[a]	0.2%	0.3%	0.5%	0.4%	0.2%	0.1%
Inerts (N_2, etc.)	2.0%	2.0%	2.0%	2.0%	2.0%	2.0%
C_2H_4/CH_4 ratio	0.51	0.89	6.67	2.28	0.44	0.12
Gross heating value (kJ/mol)	885	953	1,041	1,011	874	841
Gross heating value (Btu/scf)	1,005	1,082	1,182	1,147	992	955
Dilution with CH_4 to meet specifications[b]	0%	0%	21%	3%	0%	0%
Fraction of H_2 removed	83%	42%	75%	84%	74%	92%
After water-gas shift reaction[c]						
Final CO	0.07%	0.07%	0.07%	0.07%	0.07%	0.07%
Final H_2	19.8%	19.9%	20.0%	20.0%	19.6%	8.3%
Final inerts (including CO_2)[d]	2.4%	2.2%	1.9%	2.6%	2.7%	4.0%

Reference[e]	A	B	B	B	B	B

[a] Vapor pressures of liquid species assumed. [b] Gross heating value between 950 and 1,150 Btu/scf, and maximum H_2 concentration of 20%. [c] Water-gas shift reaction converts CO to CO_2 and H_2; inerts include produced CO_2. [d] Assume that 95% of CO_2 is removed. [e] A: Hori et al. (1994), B: Hori et al. (2003).

We found that cases 3 and 4 fell outside the acceptable heating value range, and all cases exceeded the 20% limit on H_2 (even before conversion of CO, which further increases H_2 concentrations). As a result, removal of most of the H_2 was required; this is readily accomplished with membrane separation, since H_2 is much more permeable than all other gases found in the product mixture (Baker, 2012). Because the water-gas shift reaction also produces CO_2, the concentration of inert gases including CO_2 also becomes higher than the 4% pipeline limit; various separation techniques discussed in Sections 3.5 and 3.6 could be used to remove most of the CO_2 (we assumed 95% removal).

If after applying these processes, the resulting gas mixture still fails to fulfill heating value requirements, blending with various amounts of CH_4 from pipeline gas will allow these mixtures to meet pipeline specifications, and in addition, will allow more of the H_2 to be utilized. Four of the six cases needed no blending and could in principle be injected directly (after water-gas shift treatment and H_2 and CO_2 separations) into the natural gas network, provided it could tolerate nearly 20% H_2. If the H_2 concentration limit is lower (e.g., 10%), then cases 2-4 would need some dilution with pure CH_4 (between 10% and 46%), but the others could still be used "as is." Even for case 3, with nearly 50% natural gas dilution, a great deal of synthetic CH_4 could still be utilized, with significant benefits for global GHG emissions.

6 CO_2 source considerations for net energy balance

Up until now, we have considered the energy requirements for product separation. Another key concern in designing a CO_2RR system is the source of CO_2, as unlike water in most regions,[×] providing it could require substantial amounts of energy, and could also result in substantial net GHG emissions, undermining the goal of developing alternatives to fossil fuels. While others have also examined the possible sources of CO_2 for synthetic fuels (e.g., Graves et al., 2011; van der Giesen et al., 2014), to our knowledge we present the most comprehensive assessment of CO_2 sources to date, along with separation energy estimates.

In general, CO_2 sources that could be considered as feedstocks include (see Figure 5):

1. Pure CO_2 from underground reservoirs (currently used for beverage carbonation, enhanced oil recovery and other industrial CO_2 needs).
2. Concentrated CO_2 captured from flue gas (exhaust) from fossil fuel-fired power plants, cement kilns or other industrial facilities using CCS technology. Nearly pure CO_2 is available at elevated pressures, including as a supercritical fluid above 74 bar (~1,100 psi).

Ecoinvent (2012) estimates that 0.006 MJ/kg is required to produce municipal water in Europe, and 0.012 MJ/kg for ultrapure water globally.

3. Raw flue gas from fossil-fueled industrial facilities. Flue gas from power plants contains ~3-15% CO_2 (Lackner, 2009) diluted in N_2, water vapor, trace O_2 and various impurities; flue gas from other facilities is similar. Pressures are near-atmospheric but temperatures can exceed 100 °C.
4. CO_2 emitted from fossil fuel (e.g., natural gas, petroleum) extraction operations.
5. Concentrated CO_2 captured from flue gases from biomass-fueled facilities, including biofuel production plants (e.g., fermentation-based ethanol). Composition and properties are similar to those of fossil fuel-based flue gases.
6. Raw flue gas from biomass-fueled facilities.
7. CO_2 contained in raw biogas (~50% by volume) that is typically separated and vented.
8. Direct use of atmospheric CO_2 at ~400 ppm, used raw or compressed. Major diluents are N_2, O_2, water vapor and dust.
9. Direct air CO_2 capture and concentration, producing nearly pure CO_2 at ~1 bar (or less).
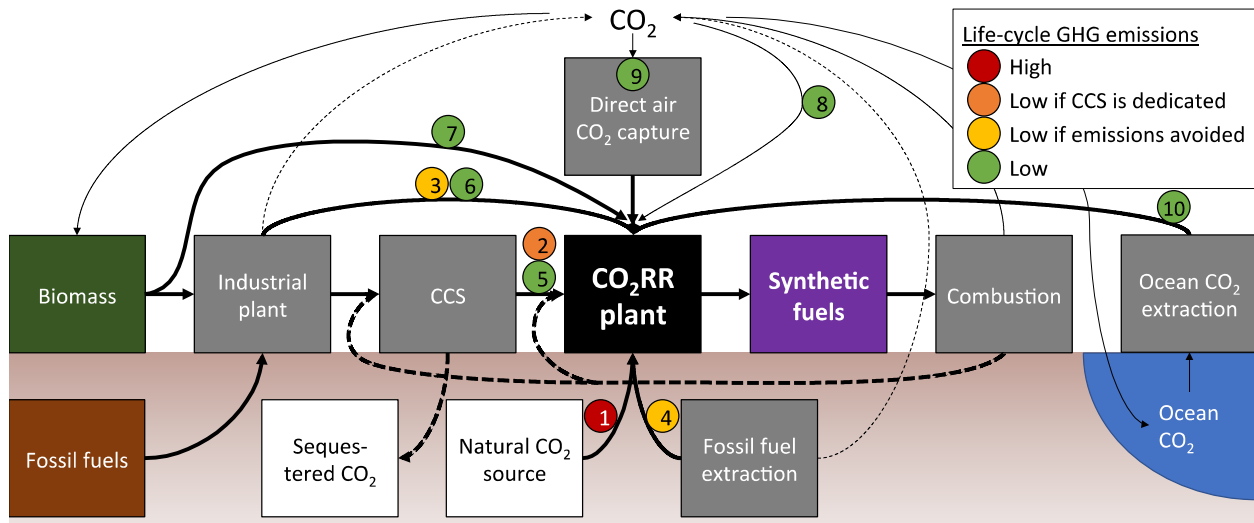10. CO_2 from seawater, producing nearly pure CO_2 at ~1 bar.

Figure 5. Potential CO_2 sources

In Table 5, we estimate the energy required to produce CO_2 from each source listed above, along with delivered pressure, and estimates of global annual CO_2 flows. Relative net CO_2 emissions are estimated from the approximate ratio of the net CO_2 emissions of a CO_2RR system utilizing the CO_2 source and combusting the resulting product fuel, to the same CO_2 source where no CO_2 is diverted to a CO_2RR plant, and an equivalent amount of fossil-derived fuel is combusted. Energy estimates are provided from sources indicated in the table. Annual CO_2 flows are based on global estimates with the exception of natural CO_2 reservoirs, where only U.S. data were available.

Table 5. Estimates the energy required to produce CO_2 from each source, along with delivered pressure, and estimates of global annual CO_2 flows

	CO_2 source	Concentration	Delivered pressure	Relative net GHG emissions[a]	Estimated separation energy	Annual global flow of source
			bar		*GJ/t CO_2*	*Gt CO_2/yr*
1	Natural CO_2	~100%	Varies	100%	~0	~0.033[b]

#	Source					
	reservoir					
2	Concentrated CO_2 from fossil fuel plant	~100%	110-200	>100% (if CCS already in place) ~50% (if CCS subsequently added)	3.5-3.9	~12-14 (power plants) ~31-34 (all fossil fuels) 2.1 (cement plants)
3	Raw flue gas from fossil fuel plant	~10-20%	1	~50%	~0	
4	Fossil fuel extraction	Varies	Varies		~0	
5	Concentrated CO_2 from biomass plant	~100%	110-200	~0%	3.5-3.9[c]	~16±4 (surface vegetation)
6	Raw flue gas from biomass plant	~10-20%	1		~0	~56-77 (biomass in 2050)
7	CO_2 in raw biogas	~50%	Varies		~0	2.8-3.8
8	Direct use from atmosphere	~0.04%	1		~0	~15
9	Concentrated CO_2 from atmosphere	~2% ~100%			0.6-6.6 1.1-13	
10	CO_2 from seawater	~100%			~2.3	~6±3

Sources are documented in Section 4 of the Supplemental Information. [a] See text for definition. [b] U.S. only [c] Assume same as for source 2

In the long term, we cannot rely on fossil energy sources to provide CO_2 for net-zero GHG fuels. As noted by Oslerloh (2016), any carbon-based technology must be closed-loop in order to be sustainable. In a future where fossil fuels are no longer combusted (or their CO_2 is captured and sequestered and not available for subsequent use), all eligible sources of CO_2 must be net zero, or result in net decrease in atmospheric and/or oceanic CO_2. Therefore, in addition to biomass as a primary source of energy and, after combustion, significant source of CO_2, the anthropogenic accumulations of CO_2 in the atmosphere (~900 Gt CO_2) and ocean (~570 Gt CO_2) are available for use (Ciais et al., 2013), with profound environmental benefits if their total concentrations can be reduced over time.

In the near term, however, using CO_2 captured from fossil power plant flue gases is a practical solution, and as noted in Section can have low net GHG emissions if the CO_2 capture is deliberately added for the benefit of CO_2RR. Because most configurations do not require highly concentrated CO_2, low pressure CO_2 (possibly including CO_2 diluted in inert gases) could be acceptable, which could significantly reduce energy requirements compared with currently-envisioned CCS systems that capture ~90% of the CO_2 in the flue gases and deliver supercritical

CO_2 to an underground storage facility. For instance, at least one research group has explored using CO_2 directly from flue gas, and observed little effect of dilution on CO_2RR (Kim et al. 2015); for GDE-based approaches, 15% CO_2 in humidified air seems adequate. For direct air capture, the required energy scales logarithmically with the change in concentration of CO_2, so roughly half the energy is needed to concentrate CO_2 from 400 ppm (ambient air) to 20,000 ppm (2 mol%), as compared with concentrating to nearly pure CO_2.

7 Energy available for separations

The energy required for separations can be obtained from several sources in the CO_2RR system: the insolation resource, combustion of unwanted products, photovoltaic electricity and co-located processing plants providing CO_2. The feasibility of obtaining sufficient energy from these sources is discussed in this section.

Although a CO_2RR method does not need to be specified for the separations discussion, some details need to be defined to consider an overall energy balance. The system assumed here is a flat-plate PEC CO_2RR system in thermal equilibrium with its surroundings in a desert setting under standard solar illumination (1000 W/m^2; NREL, no date) during the day, and in the dark at night. The cell is assumed to be thin enough that thermal gains and losses are dominated by the top and bottom surfaces. No assumptions are made about the interior configuration of the CO_2RR system, materials choices of components (other than requiring a transparent material on the sun-facing side of the cell), or the phase of electrolytes, solvents, reactants or products (see Figure 6).
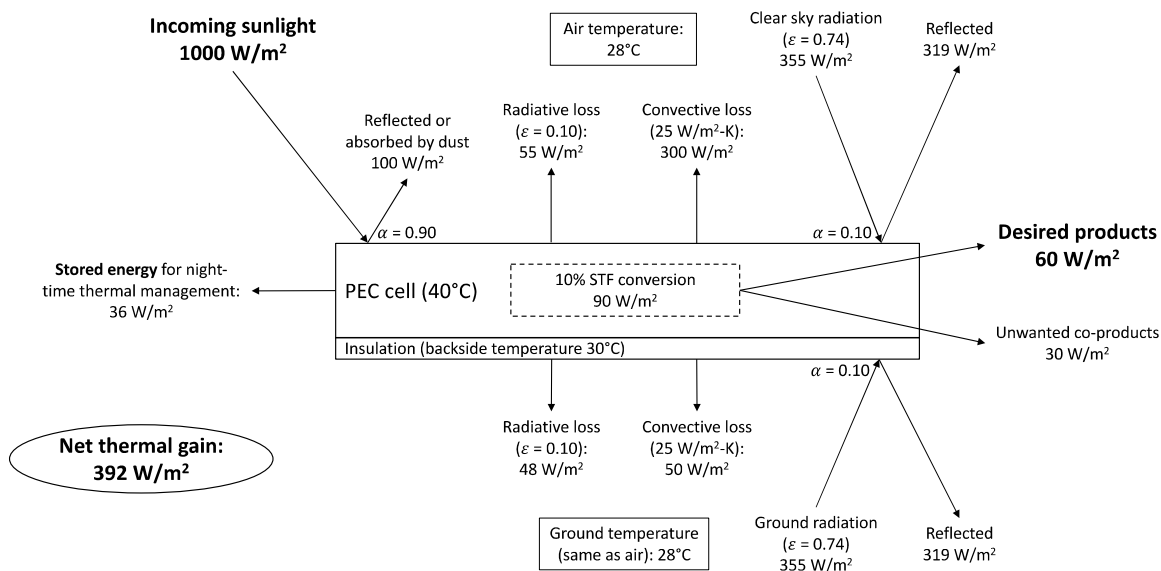

Figure 6. Energy balance of hypothetical P/EC CO_2RR system

7.1 Low-grade thermal energy from the cell

Only a small percentage of incoming solar radiation can be converted into CO_2RR products (optimistic designs target 15%); therefore, large amounts of low-grade heat are available for other uses. A simple energy-balance calculation, assuming cell operation at 40 °C and ambient air and ground temperatures of 28 °C, reveals that ~400 W/m^2 of low-grade heat energy could be made available if infrared emissivities of cell surfaces are kept low (~10%) and convective losses are managed by avoiding excessive temperature gradients. Additional thermal energy might be available from support structures, if they are coupled to a suitable heat transfer system. Note that a small amount of thermal energy (36 W/m^2) must be stored in order to manage thermal losses during nighttime (see Section 5 of the Supplemental Information for details).

However, maintaining cell operating temperatures within a reasonable range (e.g., 0 to 100 °C; Stevens and Weber, 2016) requires high heat flow, so absorbed heat must be quickly moved away from the cell and into well-insulated storage. Conversion of heat to useful energy (electricity or mechanical work) is extremely inefficient when the temperature difference is small; assuming a difference between hot (T_H) and cold (T_C) temperatures of 10% (e.g., 330 K and 300 K, respectively), the best one can expect (Carnot efficiency) is $1 - T_H/T_C$ or also 10%. As real systems can achieve only a fraction of this efficiency (~60% for efficient thermal systems and <20% for thermoelectric devices), the actual useful energy from such a heat source may therefore be ~2-6%, or ~8-24 W/m^2 assuming 392 W/m^2 of thermal energy were available. Thus, a trade-off exists between maintaining lower operating temperatures and a higher value of stored thermal energy.

Given the low expected conversion efficiencies and high convective losses under realistic conditions, it is prudent to assume that no useful energy is available from low-grade thermal energy in the cell, other than storage to manage nighttime thermal losses (which could be significant). However, other types of energy sources, discussed below, may provide useful benefits for separation.

7.2   Undesired co-products

Products other than the desired (target) product, known as co-products, could be used in a fuel cell or combustor to generate high-grade heat or additional electricity, provided they are separated efficiently from the target products. Combustion-based electrical efficiency is typically ~30-40%, but it could be boosted to ~60% if a fuel cell is used or a steam bottoming cycle is added. Combustion to produce heat is typically ~60-90% efficient, depending on the amount of heat recovery included. Thus, optimistically assuming that 70% of CO_2RR products (weighted by combustion enthalpy) is the desired fuel, 30% would be undesired co-products. Therefore, for an overall 10% efficient solar-to-product process, the combustion of co-products could provide ~10 W/m^2 of electricity or ~20-30 W/m^2 of high-grade heat. An excellent example of such a co-product would be CO or formate that, while undesirable as a commodity fuel, could still be harnessed for its high-grade heat when combusted.

Another possible use of co-products is to direct them into the anode chamber where they would be oxidized with produced O_2 for energetically favorable (and probably low cost) clean-up. This would have the added benefit of partially reducing the overpotential requirement for the anode,

increasing system performance. However, if high temperatures are needed to facilitate product separation, this would not be the best use of these co-products.

In either case, in order to minimize CO_2 emissions to the atmosphere, the CO_2 generated in the combustion process would need to be captured and re-used. This could be as straightforward as reinjecting the resulting effluent, which if burned in pure O_2 (which is also produced by the P/EC device) would be composed only of CO_2 and water, into the input side of the cell.

7.3 Waste heat from CO_2 source when collocated with CO_2RR

If flue gas from a fossil fuel- or biomass-based industrial process like a power plant is employed as a CO_2 source (see Section), substantial waste heat may be available to the P/EC system. Modern simple cycle gas turbines and many industrial thermal systems have flue gas temperatures of >500 °C. Thermal energy from this flue gas is sometimes used to drive a steam cycle to produce additional power, resulting in a flue gas temperature of ~100-200 °C. Even this low temperature exhaust could be useful if captured for use in the P/EC plant. Moreover, the amount of thermal energy contained in flue gas is several times higher than that of the CO_2 alone, because CO_2 typically comprises only ~15% of the total mass (the balance comprising N_2, water, O_2 and trace contaminants). One company (Global Thermostat) is utilizing power plant waste heat to drive the capture of CO_2 from ambient air (Global Thermostat, 2017). If collocated adjacent to CO_2-emitting power plants, the flue gas could provide ample thermal energy to drive the downstream separation process. Section 9 discusses the possibility of CO_2 sources in the deserts of the southwestern U.S., where solar insolation is expected to be highest for PEC CO_2RR.

8 Embodied energy and energy return on energy investment

The separation energy requirements and energy source considerations can be combined with estimates of the embodied energy of PEC systems to evaluate whether a CO_2RR system has the potential to be net energy positive as a product source. A detailed evaluation of a PEC water splitting installation has been described previously (Zhai et al., 2013; Sathre et al., 2014, 2016), and can be used as a reference point for PEC CO_2RR system estimates. A brief summary is provided in Section 6 of the Supplementary Information. This system, which in addition to the water-splitting device itself contained all balance-of-plant components (panel supports, water and gas handling equipment, pipes, roads, electrical tie-ins, and monitoring systems), was modeled over an assumed 40-year plant life cycle, and all energy inputs and outputs were considered. The EROEI for water splitting is defined as:

$$EROEI = \frac{T \times E_H}{E_P + T \times E_O + E_D}$$

where T = service life of the plant (years)
E_H = energy (HHV) in H_2 produced in 1 year (PJ/yr)
E_P = energy used to produce the plant (PJ)

E_O = energy used to operate the plant for 1 year (PJ/yr)
E_D = energy used to decommission the plant (PJ)

We divided the energy inputs into active PEC cell components (light absorbers, catalysts, conductive materials, membrane), inactive PEC components (encapsulation), balance of system components (panel supports, water and gas handling equipment, pipes, roads, and monitoring system), annual operations, and end-of-life decommissioning. Our overall energy calculations indicated that a plant producing 610 metric tons (t)/day H_2 (1 GW annual average) would have a 40-year lifetime energy investment of 540 PJ and energy production of 1261 PJ, for an EROEI of 2.34. That is, over 40 years the plant produces 2.34 times the energy required to construct, operate and decommission it. While positive, this value is low compared with other renewable energy systems other than U.S. corn-based ethanol (see discussion in Sathre et al., 2014), which is not surprising at this early stage of technology development.

It was well beyond the scope of this paper to estimate the embodied energies of each possible CO_2RR configuration outlined in Section 2. However, we can use the water-splitting analysis as a starting point for estimating total system energy and EROEI of a P/EC CO_2RR system, making some simple estimates of the additional embodied energy requirements of a P/EC CO_2RR system. Specifically, we consider an aqueous system with the following modifications:

- Multi-layer light-absorbing junction to provide the larger voltages required to facilitate CO_2RR
- Additional piping to provide CO_2 to the reactor and to remove liquid products (in addition to gaseous products)

The additional embodied energy required to perform the separations is not included; the estimates provided here therefore provide an upper limit to the system efficiency.

For the multi-layer light-absorbing junction, we assume the high case calculated for the water-splitting system, reflecting use of high efficiency tandem III-V light absorbers. This assumption increases the lifetime energy inputs by 78 PJ, reducing the EROEI to 2.04.

The additional embodied energy of piping will be dominated by gases; liquids require far less volume. We assume that CO_2 piping within the plant carries the gas at atmospheric pressure. Conservatively assuming that the system produces one mole of products per mole of CO_2 (e.g., exclusively C_1 products), the CO_2 piping will have the same diameters as the H_2 piping in the PEC design. If we assume that 50% of products are gases, then the required volume of piping would be equal to that of the optional O_2 products in the PEC design, carrying half the volume as that of the CO_2. For C_{2+} gases, the required volume would be less, and liquid products would require even less piping, because liquids take up much less space than gases. In total, the increase in lifetime energy inputs is 6 PJ, with a combined decrease in EROEI to 2.02.

Therefore, in order for EROEI to remain above the break-even point of one, the additional energy requirements of separation and CO_2 production, including the embodied energy of equipment, must be no greater than approximately half of the product enthalpy of combustion.

The H_2 PEC system design utilizes outside electricity inputs to provide energy for plant operations. This term appears in the denominator of the EROEI expression, and is the dominant term there, accounting for 86% of its lifetime energy use (though note that the solar energy captured and converted into H_2 is nearly three times this value). Therefore, additional energy requirements for CO_2RR systems for separations (pumping, product storage, solvent and/or membrane replacement, etc.) and CO_2 production, along with embodied energy of equipment, will further decrease the EROEI. As discussed above, this energy can vary from negligible amounts if product mixtures can be used as-is or in the case that desired products self-separate from unwanted products and solvents, to situations where the separation energy can exceed the enthalpy of the products (e.g., for dilute solutions of ethanol in water separated by distillation). If the CO_2 can be provided at no net energetic cost, and all of the required separation energy can be derived from waste energy sources (as discussed in Section 7), then the only additional term in the EROEI equation will be the embodied energy of the separation equipment, which however could still be substantial.

A far larger concern will be the overall solar-to-product conversion efficiency, which for our modeled H_2 PEC system was 10%. If a CO_2RR PEC system is only able to achieve 5% solar energy-to-desired product efficiency (e.g., Gurudayal et al., 2017), that decrease alone will lower the EROEI by a factor of two, because product energy appears in the numerator. Using the estimates provided above, this single factor would reduce the EROEI to 1.01, which means the system would barely produce more energy over its lifetime than it consumes—an unsustainable situation. Therefore, high product efficiency is of primary concern (though see Discussion section on trade-offs between product selectivity and energy available for separations).

9   Discussion

An important consideration for CO_2RR separations is that the approaches summarized in Section 3 are typically used for continuous flow operations with a constant feed. For solar-driven systems, even if products are stored overnight, the diurnal cycle suggests that constant product output would likely not be possible throughout the year, due to large seasonal fluctuations. Therefore, unless storage of raw (unseparated) products is provided on a large scale, or systems are driven continuously by non-solar resources (such as grid electricity), separation efficiencies will likely be lower due to fluctuations in product output. However, there may be an advantage in deferring the separation process until nighttime, as air temperatures tend to be cooler, boosting thermal gradients. Therefore, an advantage in separation efficiency might be realized, if unseparated products could be efficiently and inexpensively stored over half a diurnal cycle.

From the discussion of available energy for separation (Section 7), it appears that at least ~10 W/m^2 of electricity or ~20-30 W/m^2 of high-grade heat could in principle be made available from energy not used for producing target products. Moreover, copious amounts of thermal energy of at least ~100-200 °C would be available from flue gas if the CO_2RR plant were collocated adjacent to a power plant or other industrial process.

Estimates in Table 3 indicate that distillation could require anywhere from 3% to >20% of the combustion enthalpy of the target product, depending on initial concentration, desired purity, and

scale. Non-distillation approaches would consume less energy. However, if a CO_2RR system could produce ~60 W/m^2 of desired products (as assumed in Section 7), in many cases less than 10 W/m^2 of energy may be required for separation, which seems comfortably within the available resources of a well-designed, high efficiency system. It is possible that very low concentrations of desired products or multiple undesired co-products could exceed the available energy to separate them, but in most cases, it appears that no external energy sources other than sunlight might be needed to produce separated products at high purity from a CO_2RR system. However, additional embodied energy of the capital equipment necessary for these required transformations will further reduce the EROEI of such a plant.

One important trade-off to consider in designing a CO_2RR device is maximizing desired product selectivity against maximizing total product yield. While the former would appear to always be desirable, producing larger amounts of unwanted co-products for combustion could provide energy (in particular, high-grade heat) needed for separation of desired products—which could prove advantageous and even critical to ensure a high EROEI. Therefore, an optimized system might use a catalyst that produces less of the desired product but overall higher total product yield, in order to have ample energy available for separation of those products.

If pressurized sources of CO_2 are already available, it might be beneficial to utilize the excess compression energy to help drive separations, or to use it in systems that can handle high concentrations of CO_2, such as high-current EC systems or concentrated-sunlight PEC systems. Moreover, if the CO_2 source is available in close proximity to the CO_2RR plant at elevated temperature, the excess thermal energy could be used to advantage in driving separations. While collocation of a plant near CO_2 sources may not be compatible with high insolation areas, many power plants currently exist in the southwestern U.S. desert region: about 45 in Arizona and New Mexico alone, and >140 including southern California, southern Nevada, and western Texas. Together, these plants emitted 131 Mt of CO_2 in 2015 (EPA, 2016b); see Figure 7. Assuming 90% of emitted CO_2 was converted into products, this would be sufficient to produce 2.39 EJ of CH_4 (2.0% of global demand), 2.03 EJ of ethanol (6.1% of global gasoline demand), or 1.89 EJ of C_2H_4 (25% of global demand).
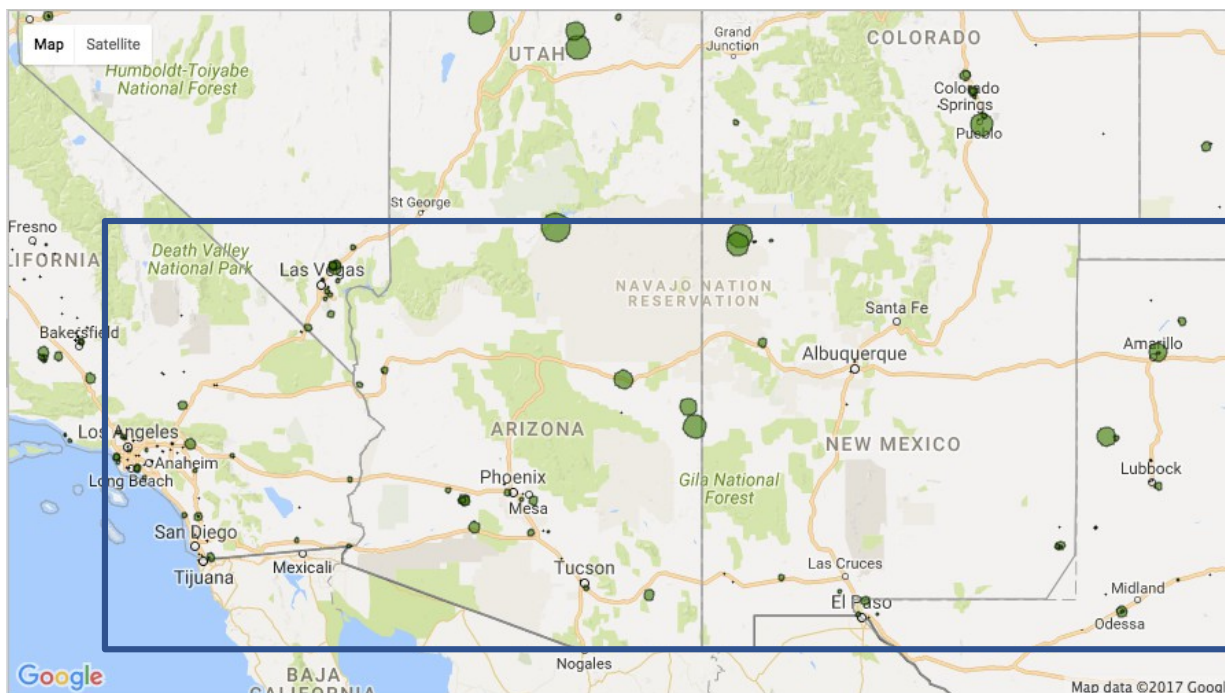
Figure 7. Map of CO_2 emissions from power plants in the desert southwestern U.S. CO_2 emissions within blue box were 131 Mt in 2015. Source: EPA (2016b).

For standalone systems, the EROEI must be as high as possible. However, if low-GHG electricity is plentiful and can be used to drive CO_2 capture when it is not otherwise needed (for instance, at midday when there is excess solar electricity, or at night when excess wind or nuclear electricity is often generated), then it might be permissible for the EROEI to be lower. Also, in order to stabilize atmospheric CO_2, it may be necessary to expend additional energy. CO_2RR should not be considered as directly competing with fossil fuels today, but rather in a future where the full externalities of fossil fuel combustion are accounted for, and other energy options including H_2 and electricity are able to fully compete in the marketplace. When fuels must be synthesized exclusively from low-GHG resources, the principal concern becomes the most sustainable and economic way of doing so, rather than whether solar fuels can compete with fossil fuels.

10 Conclusions

In this paper, we have considered a P/EC CO_2 reduction system in terms of energy return on energy invested (EROEI), that is, whether the energy embodied in chemical products would be more than the energy required to construct and operate a full system. While the CO_2 reduction technology to make products beyond CO and formate is at a very early stage, the reality that those products (alkanes, alkenes, alcohols, aldehydes and carboxylic acids) are likely to be formed in mixtures necessitates consideration of separations as an integral part of the energy balance. Product separation energy is potentially large and must be minimized, both in terms of operational as well as one-time (capital) energy investments. Based on estimates for a large-scale H_2 PEC plant, in order for the EROEI of a CO_2RR PEC plant to remain above the break-even

point, the energy requirements of separation, as well as CO_2 production and equipment embodied energies, must be no greater than approximately half of the product enthalpy of combustion—a tall challenge. If waste energy can be utilized to drive separations (or indeed other plant operations), the net energy balance and EROEI can be improved. More fundamentally, identification of catalysts that can convert CO_2 into pure or nearly pure single products would be of great benefit to the sustainability of the technology. However, the possibility of using unwanted products for combustion to produce high-grade energy (high temperatures and/or electricity) needed for product separation suggests that an optimal system may somewhat favor total product yield over high target product selectivity.

Two additional options available to improve the net energy balance have been discussed. Direct production of mixtures that are useful with only minimal post-processing will reduce the energy cost of separations. If the total energy balance is defined to include CO_2 capture, the source of CO_2 can affect energy cost. However, the required CO_2 purity and/or pressure for CO_2RR may be lower than the standards assumed for many CO_2 capture processes; if these standards can be relaxed, energy and cost savings would ensue.

Parkinson (2016) argued that the complexity and hence cost of a CO_2RR plant would be many times that of an H_2 plant, and therefore that carbon-containing fuels should be made from H_2 and CO_2, via the reverse water-gas shift and Fischer-Tropsch processes. However, a CO_2 source is needed regardless of the preferred synthesis route. We agree that if H_2 is easier to make (e.g., more practical, cheaper, efficient, net energy positive) than CO_2RR, this strategy will become the dominant pathway. But this research is still in its early stages, and it has not yet been proven that the H_2-based production route to fuels is superior to direct P/EC CO_2RR approaches.

It is evident that a focus on just one step in the P/EC conversion of CO_2 into useful products does not enable the sustainability and impacts of the technology to be accurately assessed. Progress on CO_2RR technologies requires integrated, end-to-end system designs and analyses to be developed that include energy, economic and GHG emission metrics. Moreover, by identifying the limitations of catalysis and separation, attention can be focused on the important basic science research that could advance overall progress, and dialog between the solar fuels research community and product end users as well as policymakers will be important to continued progress. Advances will enable the analysis presented here to be refined in future. While still extremely challenging, the necessity of replacing GHG-emitting fuels with net zero GHG alternatives in the 21st century makes this a compelling and worthwhile goal.

Author Contributions

All authors jointly conceptualized the paper and contributed to the original and revised drafts. J. B. G. developed the methodology, and performed most of the investigations, data analysis, and writing of the original and revised drafts. J. W. A. and D. J. M. performed the investigations for, and wrote the original drafts of, Sections 2 and 3.5, respectively.

Acknowledgments

List of acronyms

C_n	molecules containing n carbon atoms (e.g., ethylene and acetone are both C_2)
CCS	carbon dioxide capture and sequestration
CH_4	methane
C_2H_4	ethylene
C_2H_6	ethane
C_3H_6	propylene
C_3H_8	propane
CO	carbon monoxide
CO_2	carbon dioxide
CO_2RR	carbon dioxide reduction reaction
Cu	copper
EJ	exajoule (10^{18} J)
EROEI	energy return on energy invested
GDE	gas diffusion electrode
GHG	greenhouse gas
GJ	gigajoule (10^9 J)
Gt	gigaton (billion metric ton, 10^{12} kg)
H_2	hydrogen
IEA	International Energy Agency
kJ	kilojoule (1,000 J)
LLE	liquid-liquid extraction
LPG	liquefied petroleum gas
MEA	monoethanolamine
MJ	megajoule (10^6 J)
Mt	megaton (million metric ton, 10^9 kg)
MTG	methanol to gasoline
N_2	nitrogen
O_2	oxygen
PJ	petajoule (10^{15} J)
PSA	pressure-swing adsorption
SALLE	salt-assisted liquid-liquid extraction
t	metric ton (10^3 kg)

References

Acidpedia, no date. Formic Acid, http://acidpedia.org/formic_acid/. Accessed 22 September 2017.

AET (Accredited Environmental Technologies), 2010. What's that Smell? Methane. AET Insights. http://aetinc.biz/newsletters/2010-insights/october-2010. Accessed 22 September 2017.

Ager, J. W.; Shaner, M. R.; Walczak, K. A.; Sharp, I. D.; Ardo, S., 2015. Experimental demonstrations of spontaneous, solar-driven photoelectrochemical water splitting, *Energy Environ. Sci.* 8, 2811–2824.

Albo, J., M. Alvarex-Guerra, P. Castaño, A. Irabien, 2015. Towards the electrochemical conversion of carbon dioxide into methanol, *Green Chem.* 17: 2304-2342. DOI: 10.1039/c4gc02453b.

Altfeld, K., Pinchbeck D., 2013. Admissible hydrogen concentrations in natural gas systems. *Gas for energy* 2013 (3): 1-12. http://www.gerg.eu/public/uploads/files/publications/GERGpapers/SD_gfe_03_13_Report_Altfeld-Pinchbeck.pdf. Accessed 22 September 2017.

Armaroli, N., V. Balzani, 2016. Solar Electricity and Solar Fuels: Status and Perspectives in the Context of the Energy Transition, *Chem. Eur. J.* 22: 32 – 57. DOI: 10.1002/chem.201503580.

Bacher, A. D., 2016. Drying Agents, Department of Chemistry and Biochemistry, University of Calfornia, Los Angeles. http://www.chem.ucla.edu/~bacher/Specialtopics/Drying %20Agents.html. Accessed 22 September 2017.

Bachmann, J. E.; Smith, Z. P.; Li, T.; Xu, T.; and Long, J. R. Enhanced ethylene separation and plasticization resistance in polymer membranes incorporating metal–organic framework nanocrystals. *Nature Materials* 15(8) 845-849 (2016).

Badwal, S. P. S., 2013. Hydrogen production via solid electrolytic routes, *Energy and Environment* 2(5): 473-487. DOI: 10.1002/wene.50.

Baker, R. W. Future Directions of Membrane Gas Separation Technology. *Industrial and Engineering Chemistry Research* 41(6) 1393-1411 (2002).

Baker, R. W. *Membrane Technology and Applications*. Third Edition. West Sussex, UK: John Wiley & Sons, Ltd., 2012.

Baker, Richard W. and Lokhandwala, Kaaeid. Natural Gas Processing with Membranes: an Overview. *Industrial and Engineering Chemistry Research* 47(7) 2109-2121 (2008).

Baker, Richard W. and Low, Bee Ting. Gas Separation Membrane Materials: a Perspective. *Macromolecules* 47(20) 6999-7013 (2014).

Barton, E. E.; Rampulla, D. M.; Bocarsly, A. B. Selective Solar-Driven Reduction of CO2 to Methanol Using a Catalyzed P-GaP Based Photoelectrochemical Cell. J. Am. Chem. Soc. 2008, 130 (20), 6342–6344.

BASF, no date. Adsorbents for Oxygen Removal. http://adsorbents.biz/application/oxygen_removal.aspx. Accessed 22 September 2017.

BASF, 2006. n-BUTANOL, Technical Leaflet M 2084 e, BASF Petronas Chemicals, January. http://www.solvents.basf.com/portal/load/fid245442/n-BUTANOL. Accessed 22 September 2017.

Beebe, A. H., K. E. Coulter, R. A Lindsay, E. M. Baker, 1942. Equilibria in Ethanol-Water System at Pressures Less Than Atmospheric, *Industrial and Engineering Chemistry* 34(12): 1501-1504. http://pubs.acs.org/doi/pdf/10.1021/ie50396a019.

Benjaminsson G., J. Benjaminsson, R. B. Rudberg, 2013. *Power to Gas – a Technical Review*, Report SGC Rapport 2013:284, Swedish Gas Technology Center (SGC). http://www.sgc.se/ckfinder/userfiles/files/SGC284_eng.pdf. Accessed 22 September 2017.

Bender, M., 2013. Global Aromatics Supply - Today and Tomorrow, *New Technologies and Alternative Feedstocks in Petrochemistry and Refining DGMK Conference*, Dresden, Germany, October 9-11. http://www.dgmk.de/petrochemistry/abstracts_content21/Bender.pdf.

Bensmann, A., R. Hanke-Rauschenbach, R. Heyer, F. Kohrs, D. Benndorf, U. Reichl, K. Sundmacher. Biological methanation of hydrogen within biogas plants: A model-based feasibility study, *Applied Energy* 134 (2014) 413–425. DOI: 10.1016/j.apenergy.2014.08.047.

Blume, I., Wijmans, J. G., and Baker, R. W. The separation of dissolved organics from water by pervaporation. *Journal of Membrane Science* 49(3) 253-286 (1990).

Bonke, S. A.; Wiechen, M.; MacFarlane, D. R., Spiccia, L., 2015. Renewable fuels from concentrated solar power: towards practical artificial photosynthesis, *Energy Environ. Sci.* 8 (9): 2791-2796.

Bumroongsakulsawat, P.; Kelsall, G. H. Effect of Solution pH on CO: Formate Formation Rates during Electrochemical Reduction of Aqueous CO2 at Sn Cathodes. Electrochim. Acta 2014, 141, 216–225.

Burns, R. L. and Koros, W. J. Defining the challenges for C_3H_6/C_3H_8 separation using polymeric membranes. *Journal of Membrane Science* 211(2) 299-309 (2003).

Calado, J. C. G., E. J. S. Gomes De Azevedo, and V. A. M. Soares, 1980. Thermodynamic properties of binary liquid mixtures of ethane and ethylene with methane and the rare gases, *Chemical Engineering Communications* 5(1-4): 149-163,

http://www.tandfonline.com/doi/pdf/10.1080/00986448008935961. Accessed 22 September 2017.

CARB (California Air Resources Board), 2017. CARB releases major report on the future of ultra-clean and zero-emission vehicles, Press release, 18 January. https://www.arb.ca.gov/newsrel/newsrelease.php?id=890. Accessed 22 September 2017.

Carvalho, P. J., K. A. Kurnia and J. A. P. Coutinho, Dispelling some myths about the CO_2 solubility in ionic liquids, *Phys. Chem. Chem. Phys.*, 2016, 18, 14757. DOI: 10.1039/c6cp01896c

Castle, W. F., 2002. Air separation and liquefaction: recent developments and prospects for the beginning of the new millennium, *International Journal of Refrigeration* 25 (2002) 158-172.

CDC/NIOSH (The Centers for Disease Control and Prevention and The National Institute for Occupational Safety and Health), 2014. Methane. https://www.cdc.gov/niosh/ipcsneng/neng0291.html. Accessed 22 September 2017.

Cehreli, S.; Ozmen, D.; Dramur, U. 2006. (Liquid - Liquid) Equilibria of (Water + 1-Propanol + Solvent) at T = 298.2 K. *Fluid Phase Equilib.* 239, 156–160.

Centi, G. et al., 2007. Electrocatalytic conversion of CO_2 to long carbon-chain hydrocarbons, *Green Chem.* 9, 671–678. DOI: 10.1039/b615275a.

Centi, G.; Perathoner, S. 2010. Towards Solar Fuels from Water and CO_2. *ChemSusChem* 3 (2), 195–208.

Centi, G.; Perathoner, S. 2014. Perspectives and State of the Art in Producing Solar Fuels and Chemicals from CO_2. In: *Green Carbon Dioxide*; John Wiley & Sons, Inc.: Hoboken, NJ, USA, pp 1–24.

Chen, Y.; Li, C. W.; Kanan, M. W. 2012. Aqueous CO_2 Reduction at Very Low Overpotential on Oxide-Derived Au Nanoparticles. *J. Am. Chem. Soc.* 134 (49), 19969–19972.

Chong, K. C., S. O. Lai, H. S. Thiam, H. C. Teoh, S. L. Heng. 2016. Recent Progress of Oxygen/Nitrogen Separation Using Membrane Technology, *Journal of Engineering Science and Technology* 11(7): 1016 – 1030.

Ciais, P., C. Sabine, G. Bala, L. Bopp, V. Brovkin, et al., 2013: Carbon and Other Biogeochemical Cycles. In: *Climate Change 2013: The Physical Science Basis. Contribution of Working Group I to the Fifth Assessment Report of the Intergovernmental Panel on Climate Change* [Stocker, T.F., D. Qin, G.-K. Plattner, M. Tignor, S.K. Allen, et al., eds.)]. Cambridge University Press, Cambridge, United Kingdom and New York, NY, USA. http://ipcc.ch/pdf/assessment-report/ar5/wg1/WG1AR5_Chapter06_FINAL.pdf. Accessed 22 September 2017.

Clark, J., 2013. The manufacture of ethanol from ethane, Chem Guide, April. http://www.chemguide.co.uk/physical/equilibria/ethanol.html. Accessed 22 September 2017.

Corvini, G., J. Stiltner, K. Clark. No date. Mercury Removal from Natural Gas and Liquid Streams. UOP LLC, Houston, Texas, USA. https://www.uop.com/?document=mercury-removal-from-natural-gas-and-liquid-streams&download=1. Accessed 22 September 2017.

Costentin, C.; Robert, M.; Savéant, J.-M. Catalysis of the Electrochemical Reduction of Carbon Dioxide. Chem. Soc. Rev. 2013, 42 (6), 2423–2436.

Das, Mita; Koros, William J. Performance of 6FDA-6FpDA polyimide for propylene/propane separations. Journal of Membrane Science, 365(1-2) 399-408 (2010).

DeCiccio, D., S. T. Ahn, S. Sen, F. Schunk, G.T.R. Patmore, C. Rose-Petruck, Electrochemical reduction of CO_2 with clathrate hydrate electrolytes and copper foam electrodes, *Electrochem. Commun.* 52 (2015) 13–16. http://dx.doi.org/10.1016/j.elecom.2015.01.006. Accessed 22 September 2017.

Del Castillo, A.; Alvarez-Guerra, M.; Irabien, A. Continuous Electroreduction of CO_2 to Formate Using Sn Gas Diffusion Electrodes. AIChE J. 2014, 60 (10), 3557–3564.

Delacourt, C.; Newman, J. Mathematical Modeling of CO_2 Reduction to CO in Aqueous Electrolytes II. Study of an Electrolysis Cell Making Syngas ($CO+H_2$) from CO_2 and H_2O Reduction at Room Temperature. J. Electrochem. Soc. 2010, 157, B1911–B1926.

Delacourt, C.; Ridgway, P. L.; Newman, J. Mathematical Modeling of CO_2 Reduction to CO in Aqueous Electrolytes: I. Kinetic Study on Planar Silver and Gold Electrodes. J. Electrochem. Soc. 2010, 157, B1902–B1910.

Demirel, Y., 2004. *Thermodynamic Analysis of Separation Systems*, Papers in Thermal Mechanics, Paper 2, PhD thesis, University of Nebraska, Lincoln, December 1. http://digitalcommons.unl.edu/chemengthermalmech/2. Accessed 22 September 2017.

de Oliveira, M. E. D., B. E. Vaughan and E. J. J. Rykiel, Ethanol as fuel: Energy, carbon dioxide balances, and ecological footprint, *Bioscience*, 2005, 55, 593.

Dutta, A.; Rahaman, M.; Luedi, N. C.; Mohos, M.; Broekmann, P. Morphology Matters: Tuning the Product Distribution of CO 2 Electroreduction on Oxide-Derived Cu Foam Catalysts. ACS Catal. 2016, 6 (6), 3804–3814.

E3 (Energy and Environmental Economics, Inc.), 2015. *Summary of the California State Agencies' PATHWAYS Project: Long-term Greenhouse Gas Reduction Scenarios*, April 6. http://www.ethree.com/wp-content/uploads/2017/02/E3_Project_Overview_20150406.pdf. Accessed 22 September 2017.

Ecoinvent, 2012. Ecoinvent Life Cycle Inventory (LCI) database, Version 2.2. http://www.ecoinvent.ch.

Eldridge, R. B. Olefin/Paraffin Separation Technology: A Review. *Industrial & Engineering Chemistry Research* 32(10) 2208-2212 (1991).

Engineering Toolbox, no date - a. Ethanol Freeze Protected Water Solutions. http://www.engineeringtoolbox.com/ethanol-water-d_989.html. Accessed 22 September 2017.

Engineering Toolbox, no date - b. Pressure Energy: Pressure energy in a incompressible fluid. http://www.engineeringtoolbox.com/pressure-energy-d_1822.html. Accessed 22 September 2017.

EPA (U.S. Environmental Protection Agency), 2011. *Improving Biofuels Recovery Processes for Energy Efficiency and Sustainability*, Report EPA 600/F-11/018, EPA Office of Research and Development, June. https://archive.epa.gov/nrmrl/archive-std/web/pdf/p100dzkl.pdf. Accessed 22 September 2017.

EPA (U.S. Environmental Protection Agency), 2016a. NAAQS Table. https://www.epa.gov/criteria-air-pollutants/naaqs-table. Accessed 22 September 2017.

EPA, 2016b. *Facility Level Information on GHGs Tool (FLIGHT)*, Version R.115, Updated August 13. https://ghgdata.epa.gov/ghgp/main.do. Accessed 22 September 2017.

Ewing, J., 2017a. France Plans to End Sales of Gas and Diesel Cars by 2040, *New York Times,* 6 July. https://nyti.ms/2tQNBVO. Accessed 22 September 2017.

Ewing, J., 2017b. Volvo, Betting on Electric, Moves to Phase Out Conventional Engines, *New York Times*, 5 July. https://nyti.ms/2tLkF1x. Accessed 22 September 2017.

ExxonMobil. 2008. Methanol to Gasoline (MTG) Production of Clean Gasoline from Coal, Brochure, ExxonMobil Research and Engineering, Fairfax, VA. http://www.zeogas.com/files/84109525.pdf. Accessed 22 September 2017.

Fu H, Y Sun, H Teng, D Zhang, Z Xiu, 2015. Salting-out extraction of carboxylic acids, *Separation and Purification Technology* 139 (2015) 36–42. DOI: 10.1016/j.seppur.2014.11.001.

Ganesh, I. Conversion of Carbon Dioxide into Methanol - A Potential Liquid Fuel: Fundamental Challenges and Opportunities (a Review). *Renew. Sustain. Energy Rev.* 2014, 31, 221–257.

Global Thermostat, 2017. Global Thermostat: A carbon negative solution. http://globalthermostat.com/. Accessed 22 September 2017.

Goeppert, A.; Czaun, M.; Jones, J.-P.; Surya Prakash, G. K.; Olah, G. A. Recycling of Carbon Dioxide to Methanol and Derived Products – Closing the Loop. *Chem. Soc. Rev*. 2014, 43 (23), 7995–8048.

Götz M. J. Lefebvre, F. Mörs, A. M. Koch, F. Graf, et al. Renewable Power-to-Gas: A technological and economic review, *Renewable Energy,* 85 (2016) 1371-1390.

Graves, C., S. D. Ebbesen, M. Mogensen, K. S. Lackner, Sustainable hydrocarbon fuels by recycling CO_2 and H_2O with renewable or nuclear energy, *Renewable and Sustainable Energy Reviews* 15 (2011) 1–23.

Green, Don W. and Perry, Robert H. *Perry's Chemical Engineer's Handbook.* 8th Ed. New York: McGraw-Hill Professional Publishing, 2007.

Greenblatt, J. B., N. R. Brown, R. Slaybaugh, T. Wilks, E. Stewart, S. T. McCoy, The Future of Low-Carbon Electricity, *Annu. Rev. Environ. Resour.,* 42 (2017): 6.1-6.28. DOI: 10.1146/annurev-environ-102016-061138.

Gupta, A. K., C. A. S. Hall, A review of the past and current state of EROI data, *Sustainability*, 2011, 3, 1796.

Gurudayal, G.; Bullock, J.; Srankó, D. F.; Towle, C. M.; Lum, Y.; Hettick, M.; Scott, M. C.; Javey, A.; Ager III, J. W. Efficient Solar-Driven Electrochemical CO_2 Reduction to Hydrocarbons and Oxygenates, *Energy Environ. Sci.* 2017. DOI: 10.1039/C7EE01764B.

Halvorsen, I. J. and S. Skogestad 2011. Energy efficient distillation, *Journal of Natural Gas Science and Engineering* 3: 571-580, doi:10.1016/j.jngse.2011.06.002

Handoko, A. D.; Ong, C. W.; Huang, Y.; Lee, Z. G.; Lin, L.; Panetti, G. B.; Yeo, B. S. Mechanistic Insights into the Selective Electroreduction of Carbon Dioxide to Ethylene on Cu 2 O-Derived Copper Catalysts. *J. Phys. Chem. C* 2016, acs.jpcc.6b07128.

Hasseine, A., A.-H. Meniai, M. Korichi, 2009. Salting-out effect of single salts NaCl and KCl on the LLE of the systems (water + toluene + acetone), (water + cyclohexane + 2-propanol) and (water + xylene + methanol), *Desalination* 242 (1–3): 264–276. http://www.sciencedirect.com/science/article/pii/S0011916409002318. Accessed 22 September 2017.

Helton, T., M. Hindman. 2014. Methanol to Gasoline Technology: Alternative for Liquid Fuel Production, *GTL Technology Forum 2014,* Houston, TX, 30-31 July. http://cdn.exxonmobil.com/~/media/global/files/catalyst-and-licensing/2014-1551-mtg-gtl.pdf. Accessed 22 September 2017.

Herron, J. A., J. Kim, A. A. Upadhye, G. W. Huber, C. T. Maravelias, A general framework for the assessment of solar fuels technologies, *Energy Environ. Sci.,* 2015, 8, 126. DOI: 10.1039/C4EE01958J.

Hodges, J. P., Geary W., Graham S., Hooker P. and Goff R., 2015. Injecting hydrogen into the gas network – a literature search. Research Report RR1047, Health and Safety Laboratory, Derbyshire, United Kingdom. http://www.hse.gov.uk/research/rrpdf/rr1047.pdf. Accessed 22 September 2017.

Hori, Y., H. Wakebe, T. Tsukamoto, O Koga, 1994. Electrocatalytic process of CO selectivity in electrochemical reduction of CO_2 at metal electrodes in aqueous media, *Electrochimica Acta* 39 (11/12): 1833-1839.

Hori, Y., I. Takahashi, O. Koga, N. Hoshi, 2003. Electrochemical reduction of carbon dioxide at various series of copper single crystal electrodes. *J. Mol. Catal. A*, 199, 39–47. DOI: 10.1016/S1381-1169(03)00016-5.

Hori, Y. 2008. Electrochemical CO_2 Reduction on Metal Electrodes. In Modern Aspects of Electrochemistry; Vayenas, C. G., White, R. E., Gamboa-Aldeco, M. E., Eds.; Modern Aspects of Electrochemistry; Springer New York: New York, NY, 2008; pp 89–189.

IDEX, 2017. Polysulfone Material Properties, IDEX Health and Science LLC. http://www.cidraprecisionservices.com/life-sciences-materials-polymer-materials-polysulfone.html. Accessed 22 September 2017.

IEA (International Energy Agency), World Energy Outlook 2015. http://www.worldenergyoutlook.org/weo2015/. Accessed 22 September 2017.

IEA, World Energy Outlook 2016: Executive Summary, 2016. https://www.iea.org/publications/freepublications/publication/WorldEnergyOutlook2016ExecutiveSummaryEnglish.pdf. Accessed 22 September 2017.

Indexmundi, 2017. Home > Energy. http://www.indexmundi.com/energy/. Accessed 22 September 2017.

Irtem, E.; Andreu, T.; Parra, A.; Hernández-Alonso, M. D.; García-Rodríguez, S.; Riesco-García, J. M.; Penelas-Pérez, G.; Morante, J. R. Low-Energy Formate Production from CO 2 Electroreduction Using Electrodeposited Tin on GDE. J. Mater. Chem. A 2016, 4 (35), 13582–13588.

Jhong, H.-R. "Molly"; Ma, S.; Kenis, P. J. Electrochemical Conversion of CO_2 to Useful Chemicals: Current Status, Remaining Challenges, and Future Opportunities. *Curr. Opin. Chem. Eng.* 2013, 2 (2), 191–199.

Jia, J., L. C. Seitz, J. D. Benck, Y. Huo, Y. Chen, J. W. D. Ng, T. Bilir, J. S. Harris, T. F. Jaramillo. 2016. Solar water splitting by photovoltaic-electrolysis with a solar-to-hydrogen efficiency over 30%, *Nature Communications* 7: 13237. DOI: 10.1038/ncomms13237.

Jones, J.-P.; Prakash, G. K. S.; Olah, G. A. Electrochemical CO 2 Reduction: Recent Advances and Current Trends. Isr. J. Chem. 2014, 54 (10), 1451–1466.

Kamcev, J. and Freeman, B. D. Charged Polymer Membranes for Environmental/Energy Applications. *Annual Review of Chemical and Biomolecular Engineering*. 7(1) 111-133 (2016).

Kim, B., S. Ma, H.-R. M. Jhong, P. J.A. Kenis, Influence of dilute feed and pH on electrochemical reduction of CO_2 to CO on Ag in a continuous flow electrolyzer, Electrochimica Acta 166 (2015) 271–276. DOI: 10.1016/j.electacta.2015.03.064.

Kiss AA, SJ Flores Landaeta, CA Infante Ferreira, 2012. Towards energy efficient distillation technologies — Making the right choice. Energy 47 (2012) 531-542. DOI: 10.1016/j.energy.2012.09.038.

Kopljar, D.; Inan, A.; Vindayer, P.; Wagner, N.; Klemm, E. Electrochemical Reduction of CO2 to Formate at High Current Density Using Gas Diffusion Electrodes. J. Appl. Electrochem. 2014, 44 (10), 1107–1116.

Kosaric, N., Z. Duvnjak, A. Farkas, H. Sahm, S. Bringer-Meyer, O. Goebel and D. Mayer, 2011. Ethanol, In: *Ullmann's Encyclopedia of Industrial Chemistry*, Wiley-VCH, Weinheim. DOI: 10.1002/14356007.a09_587.pub2.

Kuhl, K. P.; Cave, E. R.; Abram, D. N.; Jaramillo, T. F. New Insights into the Electrochemical Reduction of Carbon Dioxide on Metallic Copper Surfaces. Energy Environ. Sci. 2012, 5 (5), 7050–7059.

Kumar, B.; Brian, J. P.; Atla, V.; Kumari, S.; Bertram, K. A.; White, R. T.; Spurgeon, J. M. New Trends in the Development of Heterogeneous Catalysts for Electrochemical CO_2 Reduction. *Catal. Today* 2016, 270, 19–30.

Kvaalen, E., P. C. Wankat, B. A. McKenzie, 1984. Alcohol Distillation: Basic Principles, Equipment, Performance Relationships, and Safety, Purdue University, Cooperative Extension Service, AE-117. https://www.extension.purdue.edu/extmedia/ae/ae-117.html. Accessed 22 September 2017.

Lackner, K. S., 2009. Capture of carbon dioxide from ambient air, *Eur. Phys. J. Special Topics* 176: 93–106. DOI: 10.1140/epjst/e2009-01150-3.

Lane, J., 2016. Biofuels Mandates Around the World: 2016, *Biofuels Digest*, 3 January. http://www.biofuelsdigest.com/bdigest/2016/01/03/biofuels-mandates-around-the-world-2016/. Accessed 22 September 2017.

Li, C. W.; Kanan, M. W. CO_2 Reduction at Low Overpotential on Cu Electrodes Resulting from the Reduction of Thick Cu_2O Films. J. Am. Chem. Soc. 2012, 134 (17), 7231–7234.

Li, H.; Oloman, C. The Electro-Reduction of Carbon Dioxide in a Continuous Reactor. J. Appl. Electrochem. 2005, 35 (10), 955–965.

Li Q-M, Q Liu, L-M Zhang, W-X Xue, 2000. Phase Separation of n-Propanol from Water and Extraction of Cadmium(ll) Complex into n-Propanol. Journal of the Chinese Chemical Society, 47: 973-977.

Li, W. Electrocatalytic Reduction of CO_2 to Small Organic Molecule Fuels on Metal Catalysts. In ACS Symposium Series; 2010; Vol. 1056, pp 55–76.

Lim, R. J.; Xie, M.; Sk, M. A.; Lee, J.-M.; Fisher, A.; Wang, X.; Lim, K. H. A Review on the Electrochemical Reduction of CO2 in Fuel Cells, Metal Electrodes and Molecular Catalysts. Catal. Today 2014, 233, 169–180.

Liptak, A., 2017. China is planning to implement a ban on fossil fuel cars, *The Verge*, 10 September. https://www.theverge.com/2017/9/10/16284866/china-ban-fossil-fuel-cars. Accessed 22 September 2017.

Luostarinen, S., A. Normak, M. Edström. 2011. *Overview of Biogas Technology*, Baltic MANURE WP6 Energy potentials, Baltic Forum for Innovative Technologies for Sustainable Manure Management, December. http://balticmanure.odeum.com/download/Reports/baltic_manure_biogas_final_total.pdf. Accessed 22 September 2017.

Luyben, W. L., 2008, Control of the Heterogeneous Azeotropic n-Butanol/Water Distillation System, *Energy & Fuels* 22: 4249–4258. http://pubs.acs.org/doi/pdf/10.1021/ef8004064. Accessed 22 September 2017.

Machunda, R. L.; Ju, H.; Lee, J. Electrocatalytic Reduction of CO2 Gas at Sn Based Gas Diffusion Electrode. Curr. Appl. Phys. 2011, 11 (4), 986–988.

Majors, R. E., 2009. Salting-out Liquid-Liquid Extraction (SALLE), LCGC North America, 27 (7): 526–533, 1 July. http://www.chromatographyonline.com/salting-out-liquid-liquid-extraction-salle. Accessed 22 September 2017.

Martin, N., 1998. Separating Azeotropic Mixtures, *Sulzer Technical Review* 3/98: 12-15, Sulzer Chemtech, Germany. http://www.sulzer.com/br/-/media/Documents/Cross_Division/STR/1998/1998_03_12_martin_e.pdf. Accessed 22 September 2017.

McCabe, Warren, Julian C. Smith and Peter Harriott, 2001. *Unit Operations of Chemical Engineering*, 6th ed., New York: McGraw-Hill. ISBN 0070393664.

Meier-Haack, J.; Lenk, W.; Lehmann, D.; and Lunkwitz, K. Pervaporation separation of water/alcohol mixtures using composite membranes based on polyelectrolyte multilayer assemblies. *Journal of Membrane Science* 184(2) 233-243 (2001).

Melaina, M. W., Antonia O, Penev M., 2013. Blending hydrogen into natural gas pipeline networks: a review of key issues. Technical Report NREL/TP-5600-51995, National Renewable

Energy Laboratory, March. http://www.nrel.gov/docs/fy13osti/51995.pdf. Accessed 22 September 2017.

Morrow III WR, J Marano, A Hasanbeigi, E Masanet, J Sathaye, Efficiency improvement and CO_2 emission reduction potentials in the United States petroleum refining industry, Energy 93 (2015) 95-105.

MRC (Merchant Research & Consulting, Ltd.), 2014. World Formaldehyde Production to Exceed 52 Mln Tonnes in 2017, June 27. https://mcgroup.co.uk/news/20140627/formaldehyde-production-exceed-52-m. Accessed 22 September 2017.

Multi-State ZEV Task Force, 2014. Multi-State ZEV Action Plan, ZEV Program Implementation Task Force, May. http://www.nescaum.org/topics/zero-emission-vehicles/multi-state-zev-action-plan. Accessed 22 September 2017.

Moshfeghian, M., 2015. How to estimate compressor efficiency? *PetroSkills Tip of the Month*, John M. Campbell and Company, 1 July. http://www.jmcampbell.com/tip-of-the-month/2015/07/how-to-estimate-compressor-efficiency/. Accessed 22 September 2017.

Myhre, G., D. Shindell, F.-M. Bréon, W. Collins, J. Fuglestvedt, J. Huang, D. Koch, J.-F. Lamarque, D. Lee, B. Mendoza, et al. 2013. Anthropogenic and natural radiative forcing. In: *Climate change 2013: The physical science basis: Contribution of Working Group I to the fifth assessment report of the Intergovernmental Panel on Climate Change*, edited by T.F. Stocker, D. Qin, G.-K. Plattner, M. Tignor, S.K. Allen, J. Boschung, A. Nauels, Y. Xia, V. Bex and P.M. Midgley. Cambridge, England: Cambridge University Press: 659–740. www.climatechange2013.org/images/report/WG1AR5_Chapter08_FINAL.pdf. Accessed 22 September 2017.

NCBI (National Center for Biotechnology Information), no date. Formic Acid, CID=284, *PubChem Compound Database*. https://pubchem.ncbi.nlm.nih.gov/compound/284. Accessed May 15, 2017.

NETL (National Energy Technology Laboratory), no date. Conversion of methanol to gasoline, U.S. Department of Energy. https://www.netl.doe.gov/research/coal/energy-systems/gasification/gasifipedia/methanol-to-gasoline. Accessed 22 September 2017.

Newman, J.; Hoertz, P. G. G.; Bonino, C. A. A.; Trainham, J. A. A. Review: An Economic Perspective on Liquid Solar Fuels. *J. Electrochem. Soc.* 2012, 159 (10), A1722–A1729.

Newsome, D. S., 1980. The Water-Gas Shift Reaction, *Catalysis Reviews* 21:2, 275-318, DOI: 10.1080/03602458008067535.

New York Times, 2017. Britain Joins the Shift to Electric Cars, editorial, 31 July. https://nyti.ms/2hfjOkU. Accessed 22 September 2017.

NIST (National Institute of Standards and Technology), 2017. NIST Chemistry WebBook, U.S. Department of Commerce. http://webbook.nist.gov/chemistry/. Accessed 22 September 2017.

Nock, W. J., M. Walker, R. Kapoor, S. Heaven. Modeling the Water Scrubbing Process and Energy Requirements for CO_2 Capture to Upgrade Biogas to Biomethane, *Ind. Eng. Chem. Res.*, 2014, 53 (32): 12783–12792. DOI: 10.1021/ie501280p.

NREL (National Renewable Energy Laboratory), no date. Reference Solar Spectral Irradiance: Air Mass 1.5. http://rredc.nrel.gov/solar/spectra/am1.5/. Accessed 22 September 2017.

Osterloh, F., 2016. The Low Concentration of CO_2 in the Atmosphere Is an Obstacle to a Sustainable Artificial Photosynthesis Fuel Cycle Based on Carbon, *ACS Energy Letters* 1, 1060−1061. DOI: 10.1021/acsenergylett.6b00493.

Packer, J., no date. The production of methanol and gasoline, New Zealand Institute of Chemistry, http://nzic.org.nz/ChemProcesses/energy/7D.pdf. Accessed 22 September 2017.

Parkinson, B., 2016. Advantages of Solar Hydrogen Compared to Direct Carbon Dioxide Reduction for Solar Fuel Production. *ACS Energy Lett.* 1, 1057−1059. DOI: 10.1021/acsenergylett.6b00377.

Pérez-Fortes, M., E. Tzimas, 2016, Techno-economic and environmental evaluation of CO_2 utilisation for fuel production: Synthesis of methanol and formic acid, Report JRC99380, Publications Office of the European Union. DOI:10.2790/981669.

Pimentel, D. Ethanol fuels: Energy balance, economics, and environmental impacts are negative, *Nat. Resour. Res.*, 2003, 12(2), 127.

Ploegmakers, J., Adriaan R. T. Jelsma, A. G. J. van der Ham, and Kitty Nijmeijer, Economic Evaluation of Membrane Potential for Ethylene/Ethane Separation in a Retrofitted Hybrid Membrane-Distillation Plant Using Unisim Design, Ind. Eng. Chem. Res., 2013, 52 (19), pp 6524–6539. DOI: 10.1021/ie400737s.

Prakash, G. K. S.; Viva, F. A.; Olah, G. A. Electrochemical Reduction of CO2 over Sn-Nafion® Coated Electrode for a Fuel-Cell-like Device. J. Power Sources 2013, 223, 68–73.

Qiao, J.; Liu, Y.; Hong, F.; Zhang, J., 2014. A Review of Catalysts for the Electroreduction of Carbon Dioxide to Produce Low-Carbon Fuels. *Chem. Soc. Rev.* 43 (2): 631–675.

Rees, N.V., R.G. Compton, Energy Environ. Sci. 4 (2011) 403–408. DOI: 10.1039/c0ee00580k Roberts, F. Sloan, Kendra P. Kuhl, and Anders Nilsson, High Selectivity for Ethylene from Carbon Dioxide Reduction over Copper Nanocube Electrocatalysts, Angew. Chem. Int. Ed. 2015, 54, 5179 –5182. DOI: 10.1002/anie.201412214.

Ren, D.; Ang, B. S.-H.; Yeo, B. S. 2016a, Tuning the Selectivity of Carbon Dioxide Electroreduction toward Ethanol on Oxide-Derived Cu X Zn Catalysts. *ACS Catal.* 8239–8247.

Ren, D.; Wong, N. T.; Handoko, A. D.; Huang, Y.; Yeo, B. S. 2016b. Mechanistic Insights into the Enhanced Activity and Stability of Agglomerated Cu Nanocrystals for the Electrochemical Reduction of Carbon Dioxide to N -Propanol. *J. Phys. Chem. Lett.* 7 (1), 20–24.

Research and Markets, 2016. The Global Ethylene Market 2016, ID 3254257, February. http://www.researchandmarkets.com/research/2xl4dr/the_ethylene. Accessed 22 September 2017.

Roberts-Austen, W. C., 1898. The Extraction of Nickel from its Ores by the Mond Process, *Nature* 59 (1516): 63–64. DOI:10.1038/059063a0.

Rodriguez, B. A., W. J. Tenn III, 2012. Direct formation of propanol from a dilute ethylene feed via reductive-hydroformylation using homogeneous rhodium catalysts at low feed pressures, *Applied Catalysis A: General* 421–422: 161–163. DOI: 10.1016/j.apcata.2012.02.013.

Rongé, J.; Bosserez, T.; Martel, D.; Nervi, C.; Boarino, L.; Taulelle, F.; Decher, G.; Bordiga, S.; Martens, J. A., 2014. Monolithic cells for solar fuels, *Chem. Soc. Rev.* 43, 7963–7981.

Sanders, D. F.; Smith, Z. P.; Guo, R.; Robeson, L. M.; McGrath, J. E.; Paul, D. R.; Freeman, B. D. Energy-efficient polymeric gas separation membranes for a sustainable future: A review. *Polymer* 54(18) 4729-4761 (2013).

Sathre R, Scown CD, Morrow WR, Stevens JC, Sharp ID, Ager JW, Walczak K, Houle FA, Greenblatt JB. 2014. Life-cycle net energy assessment of large-scale hydrogen production via photoelectrochemical water splitting. *Energy & Environmental Science* 7: 3264-3278.

Sathre, R., J. B. Greenblatt, K. Walczak, I. D. Sharp, J. C. Stevens, J. W. Ager III, F. A. Houle, 2016. Opportunities to improve the net energy performance of photoelectrochemical water-splitting technology. *Energy & Environmental Science* 9 (3), 803-819. http://dx.doi.org/10.1039/C5EE03040D.

Saveant, J.-M.; Tard, C. Attempts to Catalyze the Electrochemical CO_2-to-Methanol Conversion by Biomimetic $2e^- + 2H^+$ Transferring Molecules. J. Am. Chem. Soc. 2016, 138 (3), 1017–1021.

Schulz, H., 1999. Short history and present trends of Fischer–Tropsch synthesis, *Applied Catalysis A: General* 186, 3–12.

Schüttauf, J.-W.; Modestino, M. A.; Chinello, E.; Lambelet, D.; Delfino, A.; Dominé, D.; Faes, A.; Despeisse, M.; Bailat, J.; Psaltis, D.; Moser, C.; Ballif, C., 2016. Solar-to-Hydrogen Production at 14.2% Efficiency with Silicon Photovoltaics and Earth-Abundant Electrocatalysts. Journal of *The Electrochemical Society* 163 (10), F1177-F1181.

Shah, D. J. and K. K. Tiwari, 1981. Effect of Salt on the Distribution of Acetic Acid between Water and Organic Solvent, *J. Chem. Eng. Data* 26 (4): 375–378. DOI: 10.1021/je00026a008.

Shaner, M. R., H. A. Atwater, N. S. Lewis, E. W. McFarland, 2016. A comparative technoeconomic analysis of renewable hydrogen production using solar energy, *Energy Environ. Sci.* 9: 2354. DOI: 10.1039/c5ee02573g.

Shi, X., H. Jeong, S. J. Oh, M. Ma, K. Zhang, J. Kwon, I. T. Choi, I. Y. Choi, H. K. Kim, J. K. Kim, J. H. Park. 2016. Unassisted photoelectrochemical water splitting exceeding 7% solar-to-hydrogen conversion efficiency using photon recycling, *Nature Communications* 7: 11943. DOI: 10.1038/ncomms11943.

Shibata, H., et al., 2008. Enabling Electrocatalytic Fischer–Tropsch Synthesis from Carbon Dioxide Over Copper-based Electrodes, *Catal. Lett.* 123:186–192 DOI 10.1007/s10562-008-9488-3.

Sigma-Aldrich, 2017. Molecular Sieves - Technical Information Bulletin. http://www.sigmaaldrich.com/chemistry/chemical-synthesis/learning-center/technical-bulletins/al-1430/molecular-sieves.html. Accessed 22 September 2017.

Singh, M. R.; Bell, A. T. Design of an Artificial Photosynthetic System for Production of Alcohols in High Concentration from CO_2. *Energy Environ. Sci.* 2016, 9 (1), 193–199. DOI: 10.1039/c5ee02783g.

Singh, M. R., E. L. Clark, A. T. Bell, 2015. Thermodynamic and achievable efficiencies for solar-driven electrochemical reduction of carbon dioxide to transportation fuels, *Proc. Natl. Acad. Sci. USA* 112 (45): E6111–E6118. DOI: 10.1073/pnas.1519212112.

Spillman, R. W. Economics of gas separation membranes. *Chemical Engineering Progress* 85(1) 41-62.

Staudt-Bickel, C. and Koros, W. J. Olefin/paraffin gas separations with 6FDA-based polyimide membranes. *Journal of Membrane Science* 170(2) 205-214 (2000).

Stevens, J. C., A. Z. Weber, 2016. A Computational Study of Optically Concentrating, Solar-Fuels Generators from Annual Thermal- and Fuel-Production Efficiency Perspectives, *Journal of The Electrochemical Society*, 163 (7) H475-H484.

Stoicescu C., et al., 2011, Liquid-Liquid Phase Equilibria of 1-Propanol + Water + n-Alcohol Ternary Systems at 298.15 K and Atmospheric Pressure, DOI: 10.1021/je2002539.

Studt, F., I. Sharafutdinov, F. Abild-Pedersen, C. F. Elkjær, J. S. Hummelshøj, S. Dahl, I. Chorkendorff and J. K. Nørskov, 2014. Discovery of a Ni-Ga catalyst for carbon dioxide reduction to methanol, *Nature Chemistry* 6: 320-324. DOI: 10.1038/NCHEM.1873.

Tollefson, J., 2013. Methane leaks erode green credentials of natural gas, *Nature News*, January 2. http://www.nature.com/news/methane-leaks-erode-green-credentials-of-natural-gas-1.12123. Accessed 22 September 2017.

Tornow, C. E.; Thorson, M. R.; Ma, S.; Gewirth, A. A.; Kenis, P. J. A. Nitrogen-Based Catalysts for the Electrochemical Reduction of CO_2 to CO. J. Am. Chem. Soc. 2012, 134 (48), 19520–19523.

Tou, M., R. Michalsky, A. Steinfeld. Solar-Driven Thermochemical Splitting of CO_2 and In Situ Separation of CO and O_2 across a Ceria Redox Membrane Reactor, *Joule* 1, 146–154. DOI: 10.1016/j.joule.2017.07.015.

UNFCCC (United Nations Framework Convention on Climate Change). 2015. *Adoption of the Paris Agreement. Conference of the Parties*, Twenty-first session, FCCC/CP/2015/L.9, 12 December. https://unfccc.int/resource/docs/2015/cop21/eng/l09.pdf. Accessed 22 September 2017.

van der Giesen, C., R. Kleijn, G. J. Kramer, Energy and Climate Impacts of Producing Synthetic Hydrocarbon Fuels from CO_2, *Environ. Sci. Technol.*, 2014, 48 (12), pp 7111–7121. DOI: 10.1021/es500191g.

Wallheimer, B., 2011. Study finds more effective way to dry ethanol, reduce costs, Press release, Purdue University, Sept. 13. http://www.purdue.edu/newsroom/research/2011/110913LadischTapioca.html. Accessed 22 September 2017.

Wang, Q.; Dong, H.; Yu, H.; Yu, H. Enhanced Performance of Gas Diffusion Electrode for Electrochemical Reduction of Carbon Dioxide to Formate by Adding Polytetrafluoroethylene into Catalyst Layer. J. Power Sources 2015, 279, 1–5.

Wei, Y., et al., 2014. Comparison study on the emission characteristics of diesel- and dimethyl ether-originated particulate matters, *Applied Energy* 130:357–369. DOI: 10.1016/j.apenergy.2014.05.058.

White DC, 2012. Optimize Energy Use in Distillation. Chemical Engineering Progress, American Institute of Chemical Engineers, March, 35-41.

Windmeier, C., R. F. Barron, 2015. Joule-Thomson Effect, In: *Ullmann's Encyclopedia of Industrial Chemistry*, Wiley-VCH Verlag GmbH & Co. KGaA, Weinheim. DOI: 10.1002/14356007, ISBN: 9783527306732. http://onlinelibrary.wiley.com/store/10.1002/14356007/asset/homepages/UA_JouleThomsonEffect.pdf. Accessed 22 September 2017.

Xiao, H.; Cheng, T.; Goddard, W. A. Atomistic Mechanisms Underlying Selectivities in C 1 and C 2 Products from Electrochemical Reduction of CO on Cu(111). J. Am. Chem. Soc. 2017, 139 (1), 130–136.

Xiao, H.; Cheng, T.; Goddard, W. A.; Sundararaman, R. Mechanistic Explanation of the pH Dependence and Onset Potentials for Hydrocarbon Products from Electrochemical Reduction of CO on Cu (111). J. Am. Chem. Soc. 2016, 138 (2), 483–486.

Yampolskii, Y. Polymeric Gas Separation Membranes. *Macromolecules* 45(8) 3298-3311 (2012).

Zhai, P., S. Haussener, J. Ager, R. Sathre, K. Walczak, J. Greenblatt and T. McKone, Net primary energy balance of a solar-driven photo-electrochemical water-splitting device, *Energy & Environmental Science*, 2013, 6, 2380.

Zhang, S.; Kang, P.; Meyer, T. J. Nanostructured Tin Catalysts for Selective Electrochemical Reduction of Carbon Dioxide to Formate. J. Am. Chem. Soc. 2014, 136 (5), 1734–1737.

Zhang, Y., 2017. China Fossil Fuel Deadline Shifts Focus to Electric Car Race, *Bloomberg News*, 10 September. https://www.bloomberg.com/news/articles/2017-09-10/china-s-fossil-fuel-deadline-shifts-focus-to-electric-car-race-j7fktx9z. Accessed 22 September 2017.

Zhou, X.; Liu, R.; Sun, K.; Chen, Y.; Verlage, E.; Francis, S. A.; Lewis, N. S.; Xiang, C. Solar-Driven Reduction of 1 Atm of CO_2 to Formate at 10% Energy-Conversion Efficiency by Use of a TiO_2-Protected III–V Tandem Photoanode in Conjunction with a Bipolar Membrane and a Pd/C Cathode. ACS Energy Lett. 2016, 1 (4), 764–770.